A simplified analog of debromoaplysiatoxin lacking the B-ring of spiroketal moiety retains protein kinase C-binding and antiproliferative activities

Tomoki Sekido[a], Kosuke Yamamoto[a], Ryo C. Yanagita[b,*], Yasuhiro Kawanami[b], Yusuke Hanaki[b], and Kazuhiro Irie[c]

[a]Division of Applied Biological and Rare Sugar Sciences, Graduate School of Agriculture, Kagawa University, Kagawa 761-0795, Japan
[b]Department of Applied Biological Science, Faculty of Agriculture, Kagawa University, Kagawa 761-0795, Japan
[c]Division of Food Science and Biotechnology, Graduate School of Agriculture, Kyoto University, Kyoto 606-8502, Japan

Corresponding Author
*(R.C.Y.) E-mail: yanagita.ryo@kagawa-u.ac.jp
ORCID
Ryo C. Yanagita: 0000-0002-9217-5507

This is an Accepted Manuscript version of the following article, accepted for publication in *Bioorganic and Medicinal Chemistry*.
A simplified analog of debromoaplysiatoxin lacking the B-ring of spiroketal moiety retains protein kinase C-binding and antiproliferative activities
Tomoki Sekido, Kosuke Yamamoto, Ryo C. Yanagita, Yasuhiro Kawanami, Yusuke Hanaki, and Kazuhiro Irie
Bioorganic & Medicinal chemistry, 2022, Volume 73, Article number 116988.
`https://doi.org/10.1016/j.bmc.2022.116988`

Keywords: Aplysiatoxin; simplified analog; conformer; protein kinase C; isozyme selectivity; antiproliferative activity; molecular dynamics simulation

ABSTRACT

A simplified analog (**3**) of aplysiatoxin was synthesized. Compound **3** has only one tetrahydropyran ring at positions 3–7, the A ring of the spiroketal moiety, which is the conformation-controlling unit for the macrolactone ring. Nuclear magnetic resonance (NMR) analysis and density functional theory (DFT) calculations indicated that **3** existed as an equilibrium mixture of two conformers arising from inversion of the chair conformation of the 2,6-*trans*-tetrahydropyran ring. The des-B-ring analog **3** binds protein kinase C isozymes and exhibits antiproliferative activity toward human cancer cell lines, comparable to 18-deoxy-aplog-1 with a spiroketal moiety.

1 INTRODUCTION

Protein kinase C (PKC), a family of serine/threonine kinases,[1] plays an essential role in intracellular signaling related to cell proliferation, differentiation, and apoptosis, and is a potential target for the treatment of intractable diseases such as cancer,[2] Alzheimer's disease,[3] and acquired immunodeficiency syndrome (AIDS).[4] At least ten PKC isozymes are present in humans. These isozymes are classified into three groups based on their biological and structural properties: conventional PKCs (cPKCs: α, βI, βII, and γ), novel PKCs (δ, ε, η, and θ), and atypical PKCs (aPKCs: ζ and λ/ι).[5] 1,2-Diacyl-*sn*-glycerol (DAG), an endogenous second messenger, and tumor promoters such as 12-*O*-tetradecanoylphorbol 13-acetate (TPA), bind to the C1 domains (C1A and C1B) in the N-terminal regulatory region in cPKCs and nPKCs and activate these isozymes.[6] Activation of PKCs by tumor promoters is followed by degradation[7,8] and loss of cellular PKC proteins.[9,10] Despite being the primary targets of tumor promoters, several studies using genetically modified animal models showed that PKC isozymes act as tumor suppressors in the chemical carcinogenesis of skin.[11–15] Furthermore, a recent study showed that loss-of-function mutations occur in PKCs in many cancer cells.[16] Therefore, PKC activators that selectively activate only a subset of PKC isozymes without causing complete downregulation of entire enzymes are promising candidates for developing clinical drugs that do not exhibit undesirable effects, *e.g.*, inflammation and tumor promotion.

Naturally occurring PKC ligands, including DAG and TPA, do not exhibit isozyme selectivity.[17,18] Notably, several groups have reported synthetic ligands with moderate isozyme selectivity. For example, Cooke et al. developed AJH-836, a DAG-lactone that binds to PKCδ and ε ten times more strongly than PKCα and βII.[19] Our group also developed 1-hexyl-indolactam-V10, a ring-expanding analog of indolactam-V, which showed approximately 450-fold binding selectivity for the PKCδ-C1B domain over the PKCα-C1A domain.[20]

We recently developed a series of simplified analogs (Figure 1) of aplysiatoxin,[21–25] a marine cyanotoxin isolated from the sea hare *Stylocheilus longicauda*.[26] The 10-methyl-aplog-1 exhibited potent antiproliferative activity comparable to that of debromoaplysiatoxin toward cancer cell lines, but exhibited neither tumor-promoting nor proinflammatory activity.[23] Therefore, the 10-methyl-aplog-1 has potential as a new anticancer lead compound. Although aplysiatoxin and debromoaplysiatoxin do not selectively bind the PKC isozyme,[22,23] the 10-methyl-aplog-1 shows a certain degree of nPKC selectivity.[23,24] However, the structural factors affecting the selectivity for PKC isozymes remain unclear.

The structure of 10-methyl-aplog-1 can be divided into three regions based on the function of each region: the receptor-recognition domain at positions 1 and 25–28, the side chain at position 11, and the conformation-controlling unit at positions 2–11.[27,28] Most structural modifications on the side chain do not result in significant changes in the selectivity for PKC isozymes.[22,29,30] On the other hand, structural modification of the spiroketal moiety in the conformation-controlling unit, which forces the conformation

of the receptor-recognition domain into the active form, affects the selectivity for PKC isozymes. For example, an acetal analog (**1**, Figure 1) with an oxygen atom at position 4 instead of a carbon atom and the corresponding C3-epimer (3-*epi*-**1**, Figure 1) exhibited three- and two-fold lower selectivity for nPKCs over cPKCs than 10-methyl-aplog-1, respectively.[31] In addition, the des-A-ring analog (**2**, Figure 1) exhibited no selectivity for nPKCs.[25] Therefore, we assumed that appropriate structural modifications of the spiroketal moiety could enable the development of an analog with higher selectivity for PKC isozymes.

In this study, to elucidate the effect of B ring removal on the conformation and biological activity, a des-B-ring analog (**3**) of 18-deoxy-aplog-1[22] was synthesized. Conformational analysis of **3** and molecular dynamics (MD) simulation of **3** bound to the PKCδ-C1B domain were undertaken, and the PKC-binding ability and antiproliferative activity toward human cancer cell lines were evaluated.

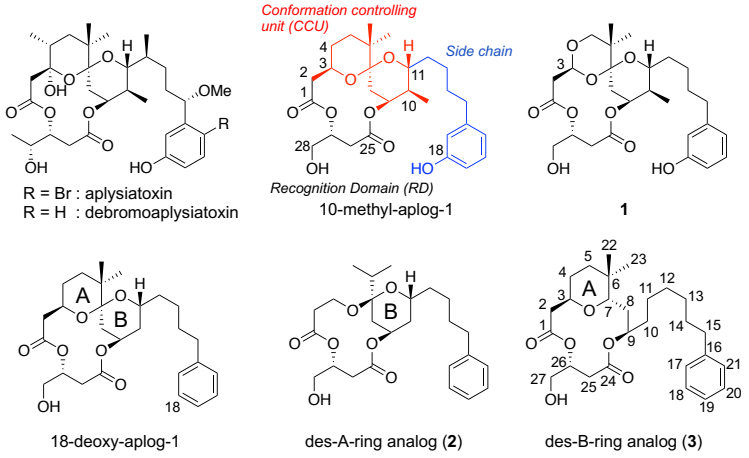

Figure 1: Structures of aplysiatoxins and corresponding simplified analogs.

2 RESULTS AND DISCUSSION

2.1 Synthesis of des-B-ring analog (3)

Retrosynthetic analysis of **3** led to a convergent synthetic route from three known intermediates: carboxylic acid **5**,[32] dithiane **8**,[21] and epoxide **9**[33] via key intermediate **4** (Scheme 1). The macrolactone core of **3** was planned to be constructed by Yamaguchi esterification[34] of the intermediate **4** and known carboxylic acid **5**, followed by macrolactonization. The 2,6-*trans*-tetrahydropyran motif in **3** and **4** is found in biologically active natural products such as leucascandrolide A, aspergillide B, phorboxazoles, and psymberin.[35] However, the asymmetric synthesis of 2,6-*trans*-tetrahydropyran remains a significant challenge due to its lower thermodynamic stability than 2,6-*cis*-tetrahydropyran. Oxy-Michael reaction and nucleophilic addition to cyclic hemiacetals via an oxocarbenium ion are often utilized to form 2,6-*trans*-tetrahydropyran,[35,36] but the steric control often requires asymmetric catalysts or neighboring group effect. In this study, we chose intramolecular Williamson ether synthesis with monomesylate **6** as a reliable and stereoselective construction of 2,6-*trans*-tetrahydropyran. A dithiane **7**, the precursor of **6**, can be derived from known intermediates, dithiane **8** and epoxide **9**, via dithiane coupling.

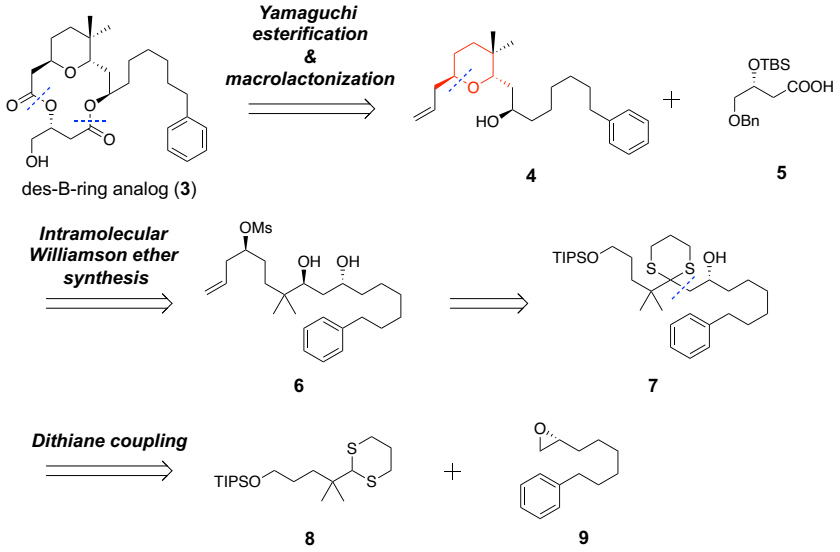

Scheme 1. Retrosynthetic analysis of **3**.

The synthesis of carboxylic acid **5** started with the coupling of benzyl (*R*)-(−)-glycidyl ether and vinylmagnesium bromide to give the known alcohol **10**[37] (Scheme 2). The secondary hydroxy group of **10** was protected as *tert*-butyldimethylsilyl (TBS) ether to give a known olefin **11**,[38] followed by oxidative cleavage of the olefin to give **5**.

The synthesis of epoxide **9** commenced with the coupling of benzyl (*R*)-(−)-glycidyl ether and 5-phenyl-1-pentyne to give alkyne **12** (Scheme 2), followed by simultaneous deprotection of the benzyl group and reduction of the alkyne via catalytic hydrogenation to give diol **13**. Regioselective sulfonation of the primary hydroxy group of **13** using 2,4,6-triisopropylbenzenesulfonyl chloride (TPS-Cl) afforded sulfonate **14**, which was treated with NaH to give **9** via intramolecular epoxidation.

The coupling of **9** with dithiane **8** afforded dithiane **7** (Scheme 3). Deprotection of the 1,3-dithiane group in the presence of iodine gave β-hydroxy ketone **15**, followed by stereoselective reduction of the keto group using the Saksena–Evans protocol[39] to provide the 1,3-diol **16**. The 1,3-diol group of **16** was protected as an acetonide to give **17**, followed by deprotection of the triisopropylsilyl (TIPS) group with tetrabutylammonium fluoride to give alcohol **18**, which was converted to aldehyde **19** by Swern oxidation.[40] The allyl group was stereoselectively installed into **19** by Keck asymmetric allylation[41] to give homoallylic alcohol **20** (>90% *de*). Mesylation of the hydroxy group of **20** with methanesulfonyl chloride gave mesylate **21**, and acid hydrolysis of the acetonide group in **21** gave monomesylate **6**.

A 2,6-*trans*-tetrahydropyran ring was stereoselectively constructed by intramolecular Williamson ether synthesis to afford alcohol **4** without byproducts such as the eight-membered cyclic ether, and a homodimer was generated. Nuclear Overhauser effect (NOE) correlations between H-8 and H-23/24, and between H-4 and H-9α were observed in a two-dimensional nuclear Overhauser effect spectroscopy (NOESY) NMR experiment in $CDCl_3$ (see Scheme 3 and Supplementary material), suggesting *trans*-configuration of the substituents at positions 4 and 8 in the tetrahydropyran ring of **4**.

The condensation of **4** with carboxylic acid **5** was achieved using Yamaguchi esterification to give **22** (Scheme 4). The TBS group of **22** was then deprotected using HF-pyridine, followed by oxidative cleavage

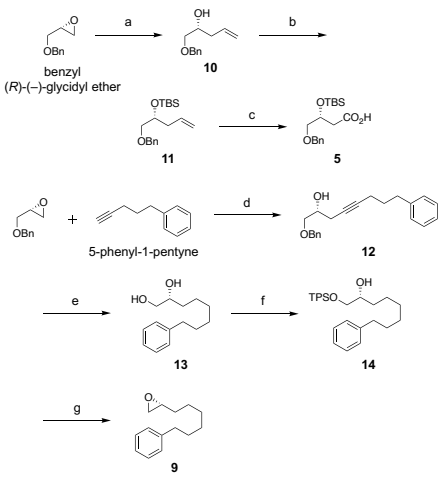

Scheme 2. Syntheses of carboxylic acid **5** and epoxide **9**.

Reagents and conditions: (a) vinylmagnesium bromide, CuI, THF, 87%; (b) *tert*-butyldimethylsilyl chloride, imidazole, DMF, 94%; (c) $NaIO_4$, $KMnO_4$, *t*-BuOH, pH 7.2 phosphate buffer, 67%; (d) *n*-BuLi, $BF_3 \cdot Et_2O$, THF, 97%; (e) H_2, 10% Pd/C, EtOH, 77%; (f) 2,4,6-triisopropylbenzenesulfonyl chloride, pyridine, 82%; (g) NaH, THF, 92%.

of an olefin to give carboxylic acid **24**. Yamaguchi macrolactonization of **24** afforded lactone **25** in 69% yield, without generating a dimer. Finally, deprotection of the benzyl group via catalytic hydrogenation gave **3** in a 19-step longest linear sequence from benzyl (*R*)-(−)-glycidyl ether and 5-phenyl-1-pentyne, with an overall yield of 5.2%.

2.2 NMR and conformational analyses of 3

^{1}H NMR analysis of **3** showed significant broadening of the peaks of H-2α and H-7, whereas the C-2, C-4, C-7, C-8, and C-23 peaks were broadened in the ^{13}C NMR profile (Supplementary material). These atoms are located in the 2,6-*trans*-tetrahydropyran ring (ring A) or in substituents on the ring. This peak broadening suggests that **3** exists in relatively fast equilibrium between multiple conformers, arising from inversion of the chair conformation of the 2,6-*trans*-tetrahydropyran ring. Using the simulated annealing method to generate possible conformers, a conformational search was performed to predict the stable conformers of **3**; two conformers (A and B) were selected, consistent with the NMR data.

Figure 2 shows the three-dimensional structure of the predicted conformers of A and B. The tetrahydropyran ring of conformer A had the same chair conformation as 18-deoxy-aplog-1[22] and natural aplysiatoxins,[42,43] wherein the substituents at positions 3 and 7 were in the equatorial and axial positions, respectively. In contrast, the tetrahydropyran ring of conformer B had an inverted *chair* conformation, wherein the substituents at positions 3 and 7 were in axial and equatorial positions, respectively. The NOESY spectrum of **3** in $CDCl_3$ showed correlations between H-3 and H-8α and between H-7 and H-22/23 (Figure 2B and Supplementary material), indicating the presence of conformer A. The relative stability of the two conformers was compared using molecular geometry optimization and vibrational calculations at the M06-2X/aug-cc-pVTZ level of theory.[44,45] The difference in the Gibbs free energy of conformers A and B at that level of theory was only 0.275 kcal mol^{-1}, supporting the existence of **3** as an equilibrium mixture of conformers A and B. Compound **3** was subjected to variable-temperature NMR measurements (Sup-

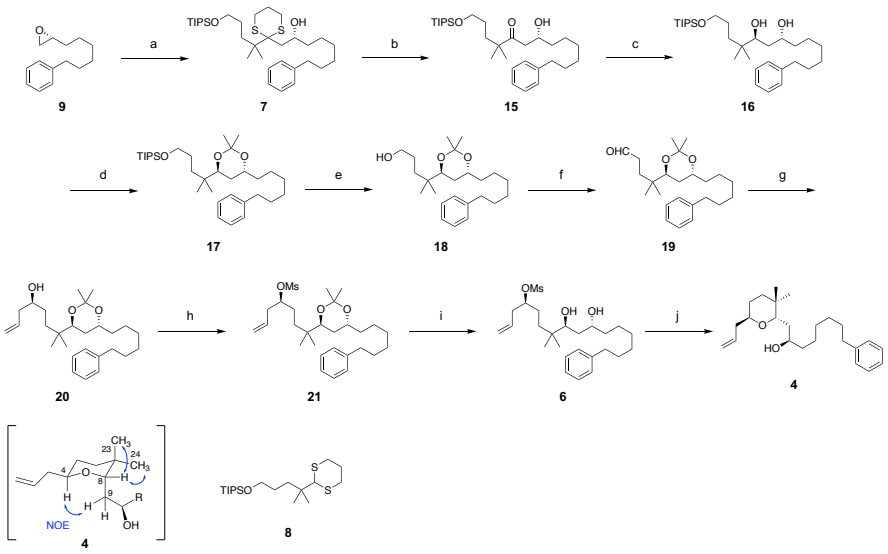

Scheme 3. Synthesis of **4**.

Reagents and conditions: (a) **8**, *n*-BuLi, THF, 92%; (b) I_2, sat. $NaHCO_3$ aq., CH_3CN, 89%; (c) $Me_4NBH(OAc)_3$, AcOH, CH_3CN, 88%; (d) 2,2-dimethoxypropane, 10-camphorsulfonic acid, CH_2Cl_2, 83%; (e) tetrabutylammonium fluoride, THF, 98%; (f) $(COCl)_2$, DMSO, Et_3N, CH_2Cl_2, 94%; (g) (*R*)-1,1'-bi-2-naphthol, $Ti(O\textit{i}\text{-}Pr)_4$, allyl-$SnBu_3$, 4 Å molecular sieves, CH_2Cl_2, 94%; (h) methanesulfonyl chloride, $Me_3N \cdot HCl$, Et_3N, CH_2Cl_2, 87%; (i) 10% HCl aq., THF, 88%; (j) NaH, THF, 75%.

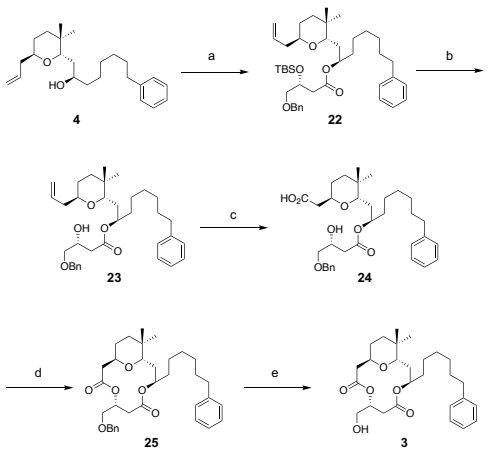

Scheme 4. Synthesis of **3**.

Reagents and conditions: (a) **5**, 2,4,6-trichlorobenzoyl chloride, Et_3N, 4-dimethylaminopyridine, toluene, 94%; (b) HF-pyridine, THF, 94%; (c) $NaIO_4$, $KMnO_4$, *t*-BuOH, pH 7.2 phosphate buffer, 74%; (d) 2,4,6-trichlorobenzoyl chloride, Et_3N, 4-dimethylaminopyridine, toluene, 69%; (e) H_2, 10% Pd/C, EtOH, 69%.

plementary material). At lower temperatures (273 and 253 K), the ^{1}H and ^{13}C peaks that broadened at room temperature (294 K) displayed further broadening. In contrast, these peaks became sharper with increasing temperature (318 and 313 K). These changes in the peak broadening suggest that **3** existed as an equilibrium mixture of the two conformers.

Figure 2C shows the superposition of the 18-deoxy-aplog-1 with conformers A and B. Even though conformer A of **3** lacks the B ring, the orientations of the two carbonyl groups in the receptor-recognition domain and the conformations of the A ring and macrolactone ring were very similar to those of 18-deoxy-aplog-1, indicating that it is possible to control the conformations of the receptor-recognition domain and macrolactone core, even with only the A ring. However, the spatial arrangement of the A ring and the orientation of the 1-carbonyl group of conformer B differed from those of 18-deoxy-aplog-1 due to inversion of the A ring (Figure 2C).

2.3 Binding ability of 3 for C1 domain of PKC isozymes

PKCα of cPKC and PKCδ of nPKC are ubiquitous isozymes and are involved in the cell-line specific antiproliferative activity of PKC ligands.[46] Thus, the selectivity of **3** for binding to the novel PKC was evaluated by examining the binding affinity for PKCα and PKCδ. Synthetic PKCα-C1A and PKCδ-C1B peptides[47] were used for the competitive binding assay because the C1A domain of cPKCs and the C1B domain of nPKCs are the main binding sites for PKC ligands.[48–51]

The half-maximal inhibitory concentration (IC_{50}) of [^{3}H]phorbol 12,13-dibutylate (PDBu) was determined using the procedure established by Sharkey and Blumberg.[52] The ability of **3** to bind the C1 peptides is expressed as the binding inhibition constant (K_i), calculated from the IC_{50} value and the dissociation constant (K_d) of [^{3}H]PDBu using the formula of Goldstein and Barrett.[53]

The K_i values of 18-deoxy-aplog-1, **2**, and **3** for α-C1A and δ-C1B are listed in Table 1. Compound **3** exhibited affinity for α-C1A (K_i = 88 nM), comparable to that of 18-deoxy-aplog-1 (K_i = 120 nM). In contrast, the affinity of **3** for δ-C1B (K_i = 17 nM) was approximately two times weaker than that of 18-deoxy-aplog-1 (K_i = 9.8 nM). Given that the binding affinity of the des-A-ring-analog (**2**) for δ-C1B was ten-fold weaker than that of 18-deoxy-aplog-1, the A ring of the spiroketal moiety, rather than the B ring, might be strongly involved in the binding of δ-C1B. The higher molecular hydrophobicity of **3** (CLogP, 4.4) compared to that of **2** (CLogP, 3.1) may also affect its selectivity for δ-C1B given that 18-deoxy-aplog-1 exhibited slightly higher selectivity for δ-C1B than aplog-1.[22] Because **3** is an equilibrium mixture of the two conformers (Figure 2A), the binding ability of each conformer was predicted using MD simulations.

Table 1: K_i values for the inhibition of [^{3}H]PDBu binding by 18-deoxy-Aplog-1, **1**, **2**, **4**, and **18**.

	K_i (nM)		
PKC C1 peptides	18-Deoxy-aplog-1[a]	**2**[b]	**3**
α-C1A	120	100	88[c] (80–95)[d]
δ-C1B	9.8	130	17[c] (12–23)[d]
Ratio (α-C1A/δ-C1B)	12	0.8	5.2
ClogP[e]	2.9	3.1	4.4

[a] Data from Ref. 22. [b] Data from Ref. 25. [c] Mean values from two independent experiments (triplicate for each ligand concentration). [d] 95% confidence intervals. [e] Calculated using ChemDraw 20.0.

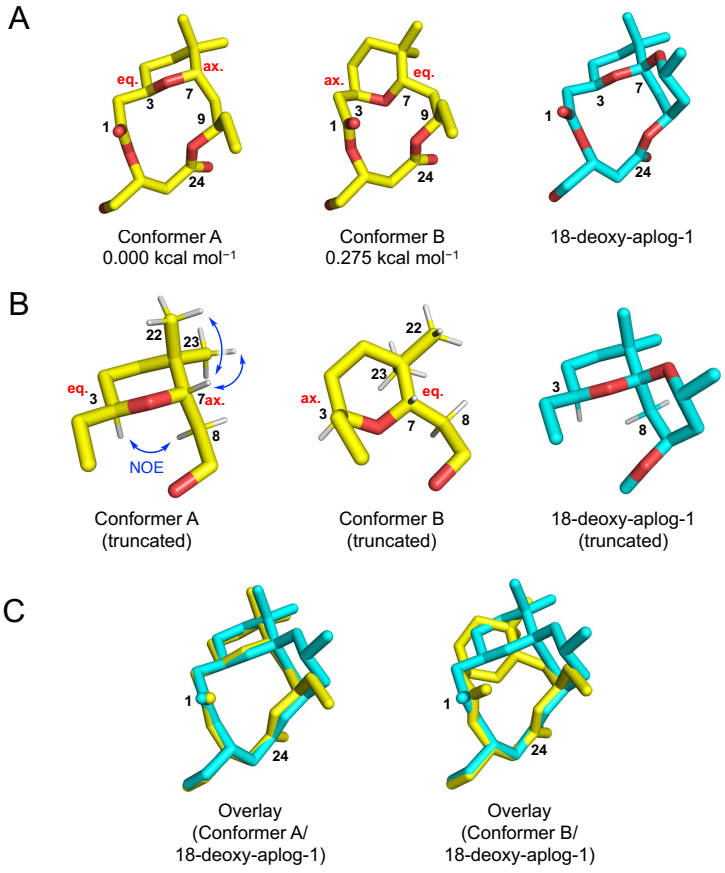

Figure 2: Three-dimensional (3D) structures of the macrolactone core of **3** and 18-deoxy-aplog-1. (A) Left and center: predicted energetically stable conformers of macrolactone core of **3** and relative energies of these conformers at the M06-2X/aug-cc-pVTZ level of theory with polarizable continuum model using the integral equation formalism (IEFPCM) solvent model with chloroform solvent. Right: structure of macrolactone core of 18-deoxy-aplog-1, predicted from crystal and solution structure of aplysiatoxins.[42,43] (B) Partial structures of **3** (conformer A, conformer B) and 18-deoxy-aplog-1. (C) Overlayed structures of 18-deoxy-aplog-1 (cyan) with conformers A or B (yellow).

2.4 Docking simulation and MD simulation of 3 with PKCδ-C1B domain

Of the two conformers of **3**, the spatial arrangement of the A-ring of conformer B significantly differed from that of 18-deoxy-aplog-1, and the orientation of the carbonyl group at position 1 was also slightly different (Figure 2C). Therefore, the binding mode of each of these conformers was predicted by docking and MD simulations of the membrane-embedded PKCδ-C1B domain in the complex with the two conformers of **3**. The initial structures of the **3**/PKCδ-C1B complex were created using the AutoDock program (version 4.2.6)[54] following a previously reported procedure,[30] and these structures were then embedded in a 1-palmitoyl-2-oleoylphosphatidylserine (POPS) bilayer membrane, which was used as a phosphatidylserine-rich plasma membrane model, using the CHARMM-GUI server[55] and the PPM server.[56] After MD simulation using the GROMACS program (version 2021.3),[57] the end-point binding free energy of the protein/ligand complex was calculated using the molecular mechanics Poisson-Boltzmann surface area (MM-PBSA) method. The cytosol-to-membrane transfer free energy ($\Delta G°_{transfer}$) of the protein/ligand complex was calculated using the PPM server based on the Orientations of Proteins in Membrane (OPM) database.[58] Because the MM-PBSA calculation provides the binding free energy in aqueous solution ($\Delta E_{MM\text{-}PBSA}$), the binding free energies in the presence of phospholipids ($\Delta G°_{bind}$) were calculated as the sum of $\Delta E_{MM\text{-}PBSA}$ and $\Delta G°_{transfer}$.

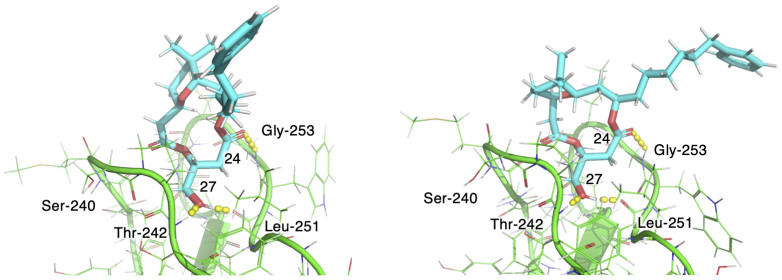

Figure 3: Predicted binding modes of conformer A (left) and conformer B (right) of **3** with the PKCδ-C1B domain. Each conformer is depicted as a stick model colored cyan (carbon), red (oxygen), and white (hydrogen). The main chain of the PKCδ-C1B domain is depicted as a cartoon and stick model colored green (carbon), red (oxygen), blue (nitrogen), and white (hydrogen). The side chains are depicted as a stick model. Yellow dashed lines represent hydrogen bonds.

Figure 3 shows a representative snapshot of the docking simulation of conformers A (left) and B (right). In these models, the carbonyl group at position 25 of both conformers formed hydrogen bonds with Gly-253, and the hydroxy group at position 27 was H-bonded to Thr-242 and Leu-251. The flexible phenylhexyl side chain at position 9 did not form a specific interaction with the protein, but were mainly involved in the interaction with the hydrophobic membrane.

Table 2 lists the predicted $\Delta G°_{bind}$ values of conformers A and B. The predicted $\Delta G°_{bind}$ of conformer A, similar to that of the 18-deoxy-aplog-1 conformation, was 2.0 kcal mol^{-1} lower than that of conformer B. Thus, the simulation indicated that conformer A has higher affinity for the PKCδ-C1B domain than conformer B. Figure 4 shows the energy decomposition per residue for van der Waals and electrostatic terms. Although there was no significant difference between conformers A and B in the electrostatic terms with hydrogen-bond forming residues (Thr-242, Leu-251, and Gly-253), the electrostatic term between the conformer A and Ser-240 was 0.943 kcal mol^{-1} lower than that of conformer B. This weaker electrostatic interaction between conformer B and Ser-240 can be attributed to the steric hindrance between the

Table 2: Predicted $\Delta E_{MM\text{-}PBSA}$, $\Delta G°_{transfer}$, and $\Delta G°_{bind}$ values of conformers A and B of **3** for the PKCδ-C1B

	$\Delta E_{MM\text{-}PBSA}$ (A)	$\Delta G°_{transfer}$ (B)[b]	$\Delta G°_{bind}$ (A+B)	
Conformer A	−9.4245 (1.0246)[a]	−12.36 (0.3)[a]	−21.8 (1.1)	(kcal mol^{-1})
Conformer B	−6.1754 (1.0298)[a]	−13.67 (0.3)[a]	−19.8 (1.1)	(kcal mol^{-1})

[a] Standard error of the mean: $n = 1000$ for A and $n = 25$ for B. [b] Calculated using PPM server and program.[58]

dimethyltetrahydropyran moiety in conformer B and the binding cleft-forming loop, which would distance the 1-carbonyl group of conformer B from Ser-240.

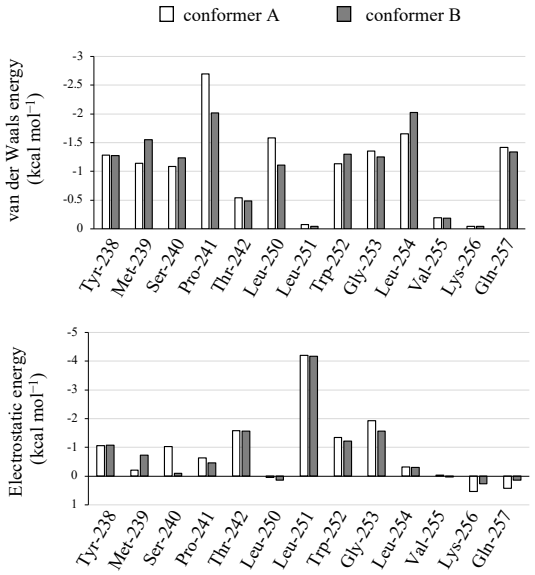

Figure 4: Decomposition of van der Waals and electrostatic energies from the MD simulation between conformer A or B and PKCδ C1B domain per residue. Values for residues that form ligand-binding cleft are shown.

2.5 Antiproliferative activity of 3

The antiproliferative activity of **3** was evaluated using growth inhibition tests for a panel of 39 human cancer cell lines established by Yamori and colleagues.[59] Figure 5 shows the growth inhibition profiles and MG-MID (the mean log GI_{50} value for all 39 cell lines) values of 18-deoxy-aplog-1, **2**, and **3**. The GI_{50} values (the concentration required to inhibit cell growth by 50% compared to the untreated control) for all 39 human cancer cell lines were reported in the Supplementary material.

The des-B-ring analog **3** exhibited significant cytotoxicity ($\log GI_{50} < -5$) toward ten (HBC-4, MDA-MB-231, SF-295, HCC2998, NCI-H460, A549, DMS273, OVCAR-5, ST-4, and MKN45) of the 39 cell lines. The efficacy profiles of 18-deoxy-aplog-1 and **3** for the panel of 39 cancer cell lines showed a significant correlation (Pearson's correlation coefficient $r = 0.930$), suggesting a similar mode of action for the antiproliferative activity, *i.e.*, the activation of PKCs mediates the antiproliferative activity of 18-deoxy-aplog-1 and **3**.

In comparison, **2** without the A ring did not exhibit significant cytotoxicity toward most cell lines, except for the NCI-H460 and MKN45 cells, and **3** without the B ring exhibited antiproliferative activity comparable to that of 18-deoxy-aplog-1. Notably, the antiproliferative activity of **3** toward NCI-H460 and MKN45 cells was superior to that of 18-deoxy-aplog-1. Because the affinities of **2** and **3** for the PKCα-C1A domain were similar, the higher cytotoxicity of **3** relative to that of **2** might be mainly attributed to the higher affinity of **3** for the PKCδ isozyme compared with **2**.

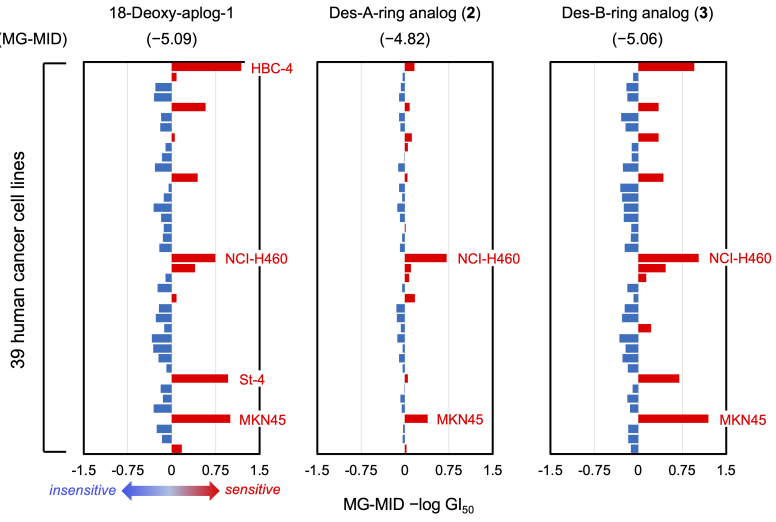

Figure 5: Graphical representation of differential growth inhibition toward a panel of 39 human cancer cell lines. Horizontal axis represents the difference between log GI_{50} for each cell line and MG-MID (mean-graph midpoint). Data for the following 39 cell lines are represented in top-to-bottom order: breast (HBC-4, BSY-1, HBC-5, MCF-7, MDA-MB-231); central nervous system (U251, SF-268, SF-295, SF-539, SNB-75, SNB-78); colon (HCC2998, KM-12, HT-29, HCT-15, HCT-116); lung (NCI-H23, NCI-H226, NCI-H522, NCI-H460, A549, DMS273, DMS114); melanoma (LOX-IMVI); ovarian (OVCAR-3, OVCAR 4, OVCAR-5, OVCAR-8, SK-OV-3); renal (RXF-631L, ACHN); stomach (St-4, MKN1, MKN-B, MKN-A, MKN45, MKN74); and prostate (DU-145, PC-3). Data for 18-deoxy-aplog-1 and **2** were cited from Ref. 22 and Ref. 25, respectively.

3 Conclusion

Based on the assumption that structural modification of the spiroketal moiety in the conformation-controlling unit affects the selectivity of PKC isozymes, a des-B-ring analog (**3**) of 18-deoxy-aplog-1 was synthesized

to reveal the effect of B-ring removal on the conformation and biological activity. Conformational analysis suggests that **3** exists as an equilibrium mixture of the two conformers. MD simulation of **3** bound to the PKCδ-C1B domain suggests that the natural product-type conformer has higher affinity for the PKCδ-C1B domain than the other conformer. Although the affinity of **3** for the PKCδ-C1B domain is slightly weaker than that of 18-deoxy-aplog-1, the affinity of **3** for the PKCα-C1A domain is comparable to that of 18-deoxy-aplog-1. Given that removal of the A ring from 18-deoxy-aplog-1 resulted in a significant decrease in the affinity for nPKCs,[25] it is deduced that the C1B domains of nPKCs more strongly recognize the A ring of the spiroketal moiety of aplysiatoxins than the B ring. The efficacy profile of **3** toward a panel of 39 human cancer cell lines is significantly correlated with that of 18-deoxy-aplog-1, suggesting that the presence of the A ring is essential for developing aplysiatoxin analogs with nPKC selectivity. This knowledge will aid the development of analogs with higher PKC isozyme selectivity in order to elucidate the complex functions of individual PKC isozymes in biological events, such as tumor promotion, apoptosis, and reactivation of latent HIV.

4 Experimental

4.1 General remarks

All moisture sensitive reactions were carried out under a positive atmosphere of argon in dried glassware. Reactions were monitored by thin-layer chromatography (TLC) using aluminum-backed silica plates coated with a 0.25 mm thickness of silica gel 60 F254 (EMD Millipore Corp., Darmstadt, Germany). Visualization was done by UV light (254 nm), followed by exposure to *p*-anisaldehyde in ethanol containing sulfuric acid and acetic acid, and gentle heating. Flash column chromatography was performed with Wakogel C-300 silica gel (FUJIFILM Wako Pure Chemical Corp., Osaka, Japan) and Wakogel 50C18 silica gel (FUJIFILM Wako Pure Chemical Corp., Osaka, Japan). HPLC purification was carried out using a YMC-pack ODS-AM column (20 mm × 150 mm, YMC Corp., Tokyo, Japan) and a JASCO PU-4086 semi preparation pump connected to a JASCO UV-4075 UV/Vis Detector (JASCO Corp., Tokyo, Japan). NMR spectra were recorded on JEOL JNM-ENZ 500R (JEOL Ltd., Tokyo, Japan) spectrometer. ^{1}H NMR chemical shifts (δ) are reported relative to tetramethylsilane (TMS, 0 ppm) in $CDCl_3$. ^{13}C NMR chemical shifts (δ) are reported relative to the carbon resonance of $CDCl_3$ (77.0 ppm). Optical rotations were measured with JASCO P-1010 (JASCO Corporation, Tokyo, Japan) digital polarimeter. HR-ESI-TOF-MS were recorded on a Waters Xevo G2-XS Tof (Waters, Tokyo, Japan) mass spectrometer. [^{3}H]PDBu (17.16 Ci/mmol) was custom synthesized by PerkinElmer Life Science Research Products (Boston, MA, U.S.). The PKC C1 peptides were synthesized as reported previously.[47] All other chemicals and reagents were purchased from chemical companies and used without purification. Compound **8** was synthesized as reported previously.[21]

4.2 Synthetic procedures

4.2.1 (*R*)-4-(Benzyloxy)-3-((*tert*-butyldimethylsilyl)oxy)butanoic acid (5)

Benzyl (*R*)-(−)-glycidyl ether (152 μL, 1.00 mmol) was treated with vinylmagnesium bromide and copper iodide in THF as reported previously[25] to afford a known alcohol **10** (168 mg, 0.873 mmol, 87%) as a colorless oil.

To a solution of **10** (251 mg, 1.31 mmol) in DMF (2.6 mL) were added imidazole (356 mg, 5.23 mmol, 4.0 equiv.) and *tert*-butyldimethylsilyl chloride (295 mg, 1.96 mmol, 1.5 equiv.), and the mixture was stirred for 6 h at room temperature. The reaction was quenched with H_2O (15 mL), and the resulting mixture was extracted with EtOAc (15 mL × 3). The combined organic layers were washed with saturated aqueous NaHCO3 and brine, dried over $MgSO_4$, filtered, and concentrated *in vacuo*. The residue was purified by column chromatography (silica gel, 3% EtOAc/hexane) to afford a known olefin **11**[38] (377 mg,

1.23 mmol, 94%) as a colorless oil.

To a suspension of $NaIO_4$ (472 mg, 2.21 mmol, 8.0 equiv.) in pH 7.2 phosphate buffer (19 mL) was added $KMnO_4$ (43.6 mg, 0.276 mmol, 1.0 equiv.) in one portion. After stirring for 15 min at room temperature, the mixture was added to a solution of olefin **11** (84.5 mg, 0.276 mmol) in *t*-BuOH (19 mL). The reaction mixture was stirred for 45 min at room temperature. The reaction was quenched with $Na_2S_2O_3$ (131 mg), and the resulting mixture was poured into EtOAc (40 mL) and H_2O (40 mL). After the organic layer was separated, the aqueous layer was extracted with EtOAc (40 mL × 2). The combined organic layers were washed with brine, dried over Na_2SO_4, filtered, and concentrated *in vacuo*. The residue was purified by column chromatography (silica gel, 15% EtOAc/hexane containing 0.1% AcOH) to afford a known carboxylic acid **5**[32] (59.5 mg, 0.183 mmol, 67%) as a colorless oil.

4.2.2 (*R*)-1-(Benzyloxy)-8-phenyloct-4-yn-2-ol (12)

To a solution of 5-phenyl-1-pentyne (1.09 g, 7.58 mmol, 2.5 equiv.) in THF (17 mL) was slowly added 1.6 M *n*-BuLi in hexane (4.6 mL, 7.4 mmol, 2.4 equiv.) over 5 min at −78 °C, and the mixture was stirred for 30 min at the same temperature. $BF_3 \cdot Et_2O$ (0.84 mL, 6.7 mmol, 2.2 equiv.) was then added to the mixture. After stirring for 30 min at −78 °C, a solution of benzyl (*R*)-(−)-glycidyl ether (506 mg, 3.08 mmol) in THF (5.8 mL) was added to the mixture at −78 °C. After stirring for 30 min at the same temperature, the reaction was quenched with saturated aqueous NH_4Cl (20 mL) and allowed to warm to room temperature. The resulting mixture was extracted with EtOAc (30 mL × 3). The combined organic layers were dried over Na_2SO_4, filtered, and concentrated *in vacuo*. The residue was purified by column chromatography (silica gel, 10% EtOAc/hexane) to afford **12** (921 mg, 2.99 mmol, 97%) as a colorless oil. $[\alpha]_D$: −9.7 (*c* 0.69, $CHCl_3$, 24.0 °C). ^{1}H NMR (500 MHz, 296 K, $CDCl_3$, 0.10 M): δ 1.79 (2H, quintet, *J* = 7.7 Hz), 2.15 (1H, dt, *J* = 7.2, 2.3 Hz), 2.17 (1H, dt, *J* = 7.2, 2.3 Hz), 2.43–2.45 (3H, m), 2.68 (2H, t, *J* = 7.7 Hz), 3.51 (1H, dd, *J* = 9.5, 6.6 Hz), 3.61 (1H, dd, *J* = 9.5, 3.7 Hz), 3.94 (1H, m), 4.57 (2H, s), 7.17–7.20 (3H, m), 7.25–7.35 (7H, m) ppm. ^{13}C NMR (125 MHz, 294 K, $CDCl_3$, 0.055 M): δ 18.2, 23.9, 30.5, 34.8, 69.2, 73.0, 73.4, 76.0, 82.4, 125.8, 127.7 (2C), 127.8, 128.3 (2C), 128.4 (2C), 128.5 (2C), 137.9, 141.6 ppm. HR-ESI-TOF-MS: *m*/*z* 331.1678 ($[MNa]^+$, calculated for $C_{21}H_{24}O_2Na$, 331.1674).

4.2.3 (*R*)-8-Phenyloctane-1,2-diol (13)

To a solution of **12** (842 mg, 2.73 mmol) in EtOH (8.4 mL) was added 10% Pd/C (89 mg). After stirring for 19 h at room temperature under H_2 atmosphere, the reaction mixture was filtered, and the filtrate was concentrated *in vacuo*. The residue was purified by column chromatography (silica gel, 50% EtOAc/hexane) to afford **13** (468 mg, 2.11 mmol, 77%) as a white crystal. $[\alpha]_D$: −0.2 (*c* 0.99, $CHCl_3$, 24.6 °C). ^{1}H NMR (500 MHz, 294 K, $CDCl_3$, 0.089 M): δ 1.34–1.46 (8H, m), 1.60–1.63 (2H, m), 2.11 (1H, br s), 2.21 (1H, br s), 2.60 (2H, t, *J* = 7.7 Hz), 3.42 (1H, m), 3.63–3.69 (2H, m), 7.16–7.18 (3H, m), 7.26–7.29 (2H, m) ppm. ^{13}C NMR (125 MHz, 294 K, $CDCl_3$, 0.089 M): δ 25.4, 29.1, 29.5, 31.4, 33.1, 35.9, 66.8, 72.3, 125.6, 128.2 (2C), 128.4 (2C), 142.7 ppm. HR-ESI-TOF-MS: *m*/*z* 245.1508 ($[MNa]^+$, calculated for $C_{14}H_{22}O_2Na$, 245.1517).

4.2.4 (*R*)-2-Hydroxy-8-phenyloctyl 2,4,6-triisopropylbenzenesulfonate (14)

To a solution of **13** (455 mg, 2.05 mmol) in pyridine (13 mL) was added 2,4,6-triisopropylbenzenesulfonyl chloride (TPS-Cl, 1.86 g, 6.14 mmol, 3.0 equiv.) at 0 °C, and the reaction mixture was allowed to warm to room temperature. After stirring for 48 h at room temperature, the reaction was quenched with H_2O (20 mL), and the resulting mixture was extracted with Et_2O (30 mL × 3). The combined organic layers were washed with brine, dried over Na_2SO_4, filtered, and concentrated *in vacuo*. The residue was purified by column chromatography (silica gel, 10% EtOAc/hexane) to afford **14** (822 mg, 1.68 mmol, 82%) as

a colorless oil. $[\alpha]_D$: −4.2 (*c* 0.92, $CHCl_3$, 24.9 °C). ^{1}H NMR (500 MHz, 295 K, $CDCl_3$, 0.041 M): δ 1.25–1.36 (23H, m), 1.39–1.45 (3H, m), 1.56–1.61 (2H, m), 2.08 (1H, d, *J* = 4.4 Hz, OH), 2.59 (2H, t, *J* = 7.7 Hz), 2.91 (1H, septet, *J* = 6.9 Hz), 3.88 (1H, m), 3.93 (1H, dd, *J* = 9.7, 7.5 Hz), 4.06 (1H, dd, *J* = 9.4, 2.5 Hz), 4.13 (2H, septet, *J* = 6.7 Hz), 7.15–7.19 (4H, m), 7.25–7.28 (3H, m) ppm. ^{13}C NMR (125 MHz, 295 K, $CDCl_3$, 0.041 M): δ 23.5 (2C), 24.7 (2C), 24.7 (2C), 25.2, 29.1, 29.3, 29.7 (2C), 31.3, 32.7, 34.2, 35.9, 69.7, 73.0, 123.8 (2C), 125.6, 128.2 (2C), 128.4 (2C), 129.1, 142.7, 150.8 (2C), 153.9 ppm. HR-ESI-TOF-MS: *m*/*z* 511.2866 ($[MNa]^+$, calculated for $C_{29}H_{44}O_4NaS$, 511.2858).

4.2.5 (*R*)-2-(6-Phenylhexyl)oxirane (9)

To a suspension of NaH (60% in oil, 269 mg, 6.72 mmol, 4.0 equiv., washed with hexane (1 mL × 3)) in THF (13 mL) was added a solution of **14** (822 mg, 1.68 mmol) in THF (6.0 mL) at 0 °C. The mixture was allowed to warm to room temperature and stirred for 2 h. The reaction was quenched with saturated aqueous NH_4Cl (18 mL), and the resulting mixture was extracted with Et_2O (20 mL × 3). The combined organic layers were washed with brine, dried over Na_2SO_4, filtered, and concentrated *in vacuo*. The residue was purified by column chromatography (silica gel, 5% EtOAc/hexane) to afford a known epoxide **9**[33] (314 mg, 1.54 mmol, 92%) as a colorless oil.

4.2.6 (*R*)-1-(2-(2-Methyl-5-((triisopropylsilyl)oxy)pentan-2-yl)-1,3-dithian-2-yl)-8-phenyloctan-2-ol (7)

To a solution of **8** (232 mg, 0.614 mmol, 3.0 equiv.) in THF (2.6 mL) was added 1.31 M *n*-BuLi in hexane (470 μL, 0.614 mmol, 1.0 equiv.) dropwise over 30 min at room temperature. A solution of **9** (40.3 mg, 0.197 mmol) in THF (1.0 mL) was then added dropwise to the reaction mixture over 30 min. After stirring for 1.5 h at room temperature, the reaction was quenched with saturated aqueous NH_4Cl (10 mL), and the resulting mixture was extracted with EtOAc (10 mL × 3). The combined organic layers were washed with brine, dried over Na_2SO_4, filtered, and concentrated *in vacuo*. The residue was purified by column chromatography (silica gel, 2%→5% EtOAc/hexane) to afford **7** (105 mg, 0.181 mmol, 92%) as a pale yellow oil. $[\alpha]_D$: +2.9 (*c* 0.56, $CHCl_3$, 23.6 °C). ^{1}H NMR (500 MHz, 296 K, $CDCl_3$, 0.043 M): δ 1.03–1.27 (27H, m), 1.33–1.39 (6H, m), 1.51–1.65 (8H, m), 1.88–2.02 (3H, m), 2.14 (1H, dd, *J* = 15.8, 9.5 Hz), 2.60 (2H, t, *J* = 7.5 Hz), 2.82–2.86 (2H, m), 2.91–2.99 (2H, m), 3.68 (2H, t, *J* = 6.3 Hz), 4.20–4.24 (2H, m), 7.15–7.18 (3H, m), 7.25–7.28 (2H, m) ppm. ^{13}C NMR (125 MHz, 296 K, $CDCl_3$, 0.043 M): δ 12.0 (3C), 18.0 (6C), 22.4, 22.5, 23.0, 25.5, 27.1, 27.3, 28.4, 29.3, 29.6, 29.7, 31.5, 32.7, 36.0, 38.5, 44.5, 45.3, 63.5, 64.0, 69.7, 125.5, 128.2 (2C), 128.4 (2C), 142.9 ppm. HR-ESI-TOF-MS: *m*/*z* 603.3714 ($[MNa]^+$, calculated for $C_{33}H_{60}O_2NaSiS_2$, 603.3702).

4.2.7 (*R*)-7-Hydroxy-4,4-dimethyl-13-phenyl-1-((triisopropylsilyl)oxy)tridecan-5-one (15)

To a solution of **7** (110 mg, 0.188 mmol) in CH_3CN (26 mL) were added a solution of I_2 (191 mg, 0.754 mmol, 4.0 equiv.) in CH_3CN (17 mL) and saturated aqueous $NaHCO_3$ (8.5 mL) at 0 °C. After stirring for 2 h at 0 °C, the reaction was quenched with saturated aqueous $NaHCO_3$ (25 mL) and 20% aqueous $Na_2S_2O_3$ (25 mL) and stirred for 10 min at room temperature. The resulting mixture was extracted with EtOAc (50 mL × 3). The combined organic layers were washed with brine, dried over Na_2SO_4, filtered, and concentrated *in vacuo*. The residue was purified by column chromatography (silica gel, 5% EtOAc/hexane) to afford **15** (82.6 mg, 0.168 mmol, 89%) as a colorless oil. $[\alpha]_D$: −17 (*c* 0.34, $CHCl_3$, 23.6 °C). ^{1}H NMR (500 MHz, 296 K, $CDCl_3$, 0.039 M): δ 1.03–1.12 (27H, m), 1.32–1.43 (10H, m), 1.56–1.63 (4H, m), 2.48 (1H, dd, *J* = 17.8, 9.5 Hz), 2.60 (2H, t, *J* = 7.5 Hz), 2.67 (1H, dd, *J* = 17.8, 2.3 Hz), 3.30 (1H, d, *J* = 2.9 Hz), 3.64–3.65 (2H, m), 3.97 (1H, m), 7.15–7.18 (3H, m), 7.25–7.28 (2H, m) ppm. ^{13}C NMR

(125 MHz, 296 K, $CDCl_3$, 0.039 M): δ 12.0 (3C), 18.0 (6C), 24.1, 24.3, 25.5, 28.2, 29.2, 29.5, 31.4, 35.9, 36.1, 36.4, 43.3, 47.6, 63.3, 67.8, 125.6, 128.2 (2C), 128.4 (2C), 142.8, 217.9 ppm. HR-ESI-TOF-MS: *m*/*z* 513.3738 ($[MNa]^+$, calculated for $C_{30}H_{54}O_3NaSi$, 513.3740).

4.2.8 (5*S*,7*R*)-4,4-Dimethyl-13-phenyl-1-((triisopropylsilyl)oxy)tridecane-5,7-diol (16)

To a solution of $Me_4NBH(OAc)_3$ (592 mg, 2.25 mmol, 6.0 equiv.) in CH_3CN (6.0 mL) was added AcOH (2.1 mL). After stirring for 30 min at room temperature, the mixture was cooled to −40 °C. A solution of **15** (185 mg, 0.376 mmol) in CH_3CN (5.0 mL) was then added to the reaction mixture, and the reaction mixture was stirred for 68 h at −30 °C. The reaction was quenched with saturated aqueous Rochelle salt (30 mL), and then resulting mixture was allowed to warm to room temperature. After stirring for 2.5 h at room temperature, saturated aqueous $NaHCO_3$ (5.0 mL) was added. The resulting mixture was extracted with EtOAc (30 mL × 3). The combined organic layers were washed with brine, dried over Na_2SO_4, filtered, and concentrated *in vacuo*. The residue was purified by column chromatography (silica gel, 10%→15% EtOAc/hexane) to afford **16** (163 mg, 0.330 mmol, 88%) as a colorless oil. $[\alpha]_D$: −7.7 (*c* 0.47, $CHCl_3$, 23.7 °C). ^{1}H NMR (500 MHz, 294 K, $CDCl_3$, 0.026 M): δ 0.85 (3H, s), 0.89 (3H, s), 1.05–1.12 (21H, m), 1.24–1.62 (18H, m), 2.14 (1H, m), 2.30 (1H, m), 2.60 (2H, t, *J* = 7.7 Hz), 3.63–3.72 (3H, m), 3.89 (1H, br s), 7.16–7.18 (3H, m), 7.26–7.29 (2H, m) ppm. ^{13}C NMR (125 MHz, 294 K, $CDCl_3$, 0.026 M): δ 12.0 (3C), 18.0 (6C), 22.8 (2C), 25.9, 27.0, 29.2, 29.5, 31.4, 34.7, 35.9, 36.6, 36.8, 37.2, 64.1, 69.9, 74.4, 125.6, 128.2 (2C), 128.4 (2C), 142.8 ppm. HR-ESI-TOF-MS: *m*/*z* 515.3903 ($[MNa]^+$, calculated for $C_{30}H_{56}O_3NaSi$, 515.3896).

4.2.9 ((4-((4*S*,6*R*)-2,2-Dimethy-6-(6-phenylhexyl)-1,3-dioxan-4-yl)-4-methylpentyl)oxy)triisopropylsilane (17)

To a solution of **16** (183 mg, 0.372 mmol) in CH_2Cl_2 (5.0 mL) were added 2,2-dimethoxypropane (1.36 mL, 11.1 mmol, 30 equiv.) and 10-camphorsulfonic acid (25.8 mg, 0.111 mmol, 0.3 equiv.), and the reaction mixture was stirred for 28 h at room temperature. The reaction was quenched with saturated aqueous $NaHCO_3$ (7.5 mL), and the resulting mixture was extracted with EtOAc (10 mL × 3). The combined organic layers were washed with brine, dried over Na_2SO_4, filtered, and concentrated *in vacuo*. The residue was purified by column chromatography (silica gel, 5%→20% EtOAc/hexane) to afford **17** (164 mg, 0.308 mmol, 83%) as a colorless oil. $[\alpha]_D$: −19 (*c* 0.32, $CHCl_3$, 23.8 °C). ^{1}H NMR (500 MHz, 295 K, $CDCl_3$, 0.032 M): δ 0.80 (3H, s), 0.84 (3H, s), 1.04–1.11 (21H, m), 1.23–1.40 (16H, m), 1.46–1.54 (3H, m), 1.60–1.63 (2H, m), 1.72 (1H, ddd, *J* = 13.2, 9.7, 5.7 Hz), 2.60 (2H, t, *J* = 7.5 Hz), 3.48 (1H, dd, *J* = 9.7, 6.3 Hz), 3.62–3.66 (3H, m), 7.15–7.18 (3H, m), 7.26–7.29 (2H, m) ppm. ^{13}C NMR (125 MHz, 295 K, $CDCl_3$, 0.032 M): δ 12.0 (3C), 18.0 (6C), 22.2, 22.4, 24.2, 24.7, 25.4, 27.4, 29.3, 29.5, 31.4, 33.6, 34.3, 35.6, 35.9, 36.0, 64.3, 67.1, 72.6, 100.0, 125.5, 128.2 (2C), 128.4 (2C), 142.9 ppm. HR-ESI-TOF-MS: *m*/*z* 555.4218 ($[MNa]^+$, calculated for $C_{33}H_{60}O_3NaSi$, 555.4209).

4.2.10 4-((4*S*,6*R*)-2,2-Dimethyl-6-(6-phenylhexyl)-1,3-dioxan-4-yl)-4-methylpentan-1-ol (18)

To a solution of **17** (155 mg, 0.290 mmol) in THF (1.3 mL) was added 1 M tetrabutylammonium fluoride in THF (350 μL, 0.348 mmol, 1.2 equiv.) at 0 °C. The mixture was allowed to warm to room temperature and stirred for 4 h. The reaction was quenched with saturated aqueous NH_4Cl (2.2 mL), and the resulting mixture was extracted with EtOAc (5 mL × 3). The combined organic layers were washed with brine, dried over Na_2SO_4, filtered, and concentrated *in vacuo*. The residue was purified by column chromatography (silica gel, 15% EtOAc/hexane) to afford **18** (107 mg, 0.285 mmol, 98%) as a colorless oil. $[\alpha]_D$: −24

(*c* 0.47, $CHCl_3$, 23.5 °C). ^{1}H NMR (500 MHz, 294 K, $CDCl_3$, 0.040 M): δ 0.81 (3H, s), 0.85 (3H, s), 1.21–1.42 (17H, m), 1.46–1.57 (3H, m), 1.59–1.61 (2H, m), 1.73 (1H, ddd, *J* = 12.6, 10.0, 5.7 Hz), 2.60 (2H, t, *J* = 7.7 Hz), 3.49 (1H, dd, *J* = 10.0, 6.3 Hz), 3.61–3.66 (3H, m), 7.16–7.18 (3H, m), 7.26–7.29 (2H, m) ppm. ^{13}C NMR (125 MHz, 294 K, $CDCl_3$, 0.040 M): δ 22.2, 22.3, 24.2, 24.7, 25.4, 27.2, 29.2, 29.4, 31.4, 33.6, 34.1, 35.6, 35.9, 36.0, 63.9, 67.1, 72.5, 100.1, 125.5, 128.2 (2C), 128.4 (2C), 142.8 ppm. HR-ESI-TOF-MS: *m*/*z* 399.2879 ($[MNa]^+$, calculated for $C_{24}H_{40}O_3Na$, 399.2875).

4.2.11 4-((4*S*,6*R*)-2,2-Dimethyl-6-(6-phenylhexyl)-1,3-dioxan-4-yl)-4-methylpentanal (19)

To a mixed solution of dimethyl sulfoxide (68 μL, 0.96 mmol, 3.5 equiv.) and CH_2Cl_2 (2.2 mL) was added $(COCl)_2$ (40 μL, 0.46 mmol, 1.7 equiv.) at −78 °C. After stirring for 30 min at −78 °C, a solution of **18** (103 mg, 0.273 mmol) in CH_2Cl_2 (0.8 mL) was added to the reaction mixture. After stirring for 3.5 h at −78 °C, triethylamine (0.38 mL, 2.7 mmol, 10 equiv.) was added to the reaction mixture, and the mixture was allowed to warm to room temperature. The resulting mixture was poured into EtOAc (10 mL) and water (10 mL). After the organic layer was separated, the aqueous layer was extracted with EtOAc (10 mL × 2). The combined organic layers were washed with brine, dried over Na_2SO_4, filtered, and concentrated *in vacuo*. The residue was purified by column chromatography (silica gel, 5% EtOAc/hexane) to afford **19** (96.5 mg, 0.258 mmol, 94%) as a colorless oil. $[\alpha]_D$: −21 (*c* 0.14, $CHCl_3$, 24.0 °C). ^{1}H NMR (500 MHz, 295 K, $CDCl_3$, 0.078 M): δ 0.82 (3H, s), 0.85 (3H, s), 1.27–1.43 (14H, m), 1.48 (1H, m), 1.54 (1H, ddd, *J* = 14.0, 10.9, 5.7 Hz), 1.60–1.63 (2H, m), 1.65 (1H, ddd, *J* = 13.8, 10.3, 5.7 Hz), 1.73 (1H, ddd, *J* = 12.6, 9.7, 5.7 Hz), 2.40 (1H, dddd, *J* = 16.9, 10.6, 5.7, 1.7 Hz), 2.46 (1H, dddd, *J* = 16.9, 10.6, 5.7, 1.7 Hz), 2.60 (2H, t, *J* = 7.7 Hz), 3.48 (1H, dd, *J* = 9.7, 6.3 Hz), 3.65 (1H, m), 7.16–7.18 (3H, m), 7.26–7.29 (2H, m), 9.78 (1H, t, *J* = 1.7 Hz) ppm. ^{13}C NMR (125 MHz, 295 K, $CDCl_3$, 0.078 M): δ 22.2, 22.5, 24.2, 24.6, 25.4, 29.2, 29.4, 30.0, 31.4, 33.5, 35.5, 35.9, 36.0, 39.2, 67.0, 72.6, 100.1, 125.5, 128.2 (2C), 128.4 (2C), 142.8, 203.1 ppm. HR-ESI-TOF-MS: *m*/*z* 397.2730 ($[MNa]^+$, calculated for $C_{24}H_{38}O_3Na$, 397.2719).

4.2.12 (*S*)-7-((4*S*,6*R*)-2,2-Dimethyl-6-(6-phenylhexyl)-1,3-dioxan-4-yl)-7-methyloct-1-en-4-ol (20)

To a suspension of (*R*)-1,1'-bi-2-naphthol ((*R*)-BINOL, 222 mg, 0.773 mmol, 3.0 equiv.) and 4 Å molecular sieves (957 mg) in CH_2Cl_2 (3.0 mL) was added $Ti(O\textit{i}\text{-}Pr)_4$ (153 μL, 0.515 mmol, 2.0 equiv.) at room temperature. The mixture was heated at reflux for 1 h. After the mixture was cooled to room temperature, a solution of **19** (96.5 mg, 0.258 mmol) in CH_2Cl_2 (1.5 mL) was added to the mixture. The mixture was stirred for 5 min at room temperature and then cooled to −78 °C. Allyl-$SnBu_3$ (1.3 mL, 4.2 mmol, 16 equiv.) was then added to the mixture. The resulting reaction mixture was kept in a freezer at −25 °C for 115 h without stirring, and then filtered. To the filtrate was added saturated aqueous $NaHCO_3$ (23 mL), and the mixture was stirred for 2 h at room temperature. The organic layer was separated, and the aqueous layer was extracted with CH_2Cl_2 (30 mL × 3). The combined organic layers were dried over Na_2SO_4, filtered, and concentrated *in vacuo*. The residue was purified by column chromatography (silica gel, 10%→15% EtOAc/hexane) to afford **20** (102 mg, 0.245 mmol, 94%) as a colorless oil. $[\alpha]_D$: −20 (*c* 0.12, $CHCl_3$, 24.0 °C). ^{1}H NMR (500 MHz, 295 K, $CDCl_3$, 0.047 M): δ 0.81 (3H, s), 0.85 (3H, s), 1.25–1.52 (19H, m), 1.60–1.63 (2H, m), 1.73 (1H, ddd, *J* = 12.7, 10.0, 5.8 Hz), 2.14 (1H, dtt, *J* = 14.0, 7.9, 0.9 Hz), 2.31 (1H, dddt, *J* = 13.9, 6.5, 4.3, 1.3 Hz), 2.60 (2H, t, *J* = 7.4 Hz), 3.49 (1H, dd, *J* = 10.0, 6.3 Hz), 3.58 (1H, m), 3.64 (1H, m), 5.12–5.17 (2H, m), 5.82 (1H, m), 7.15–7.18 (3H, m), 7.25–7.29 (2H, m) ppm. ^{13}C NMR (125 MHz, 294 K, $CDCl_3$, 0.024 M): δ 22.2, 22.5, 24.2, 24.7, 25.4, 29.2, 29.4, 30.9, 31.4, 33.5, 34.1, 35.7, 35.9, 36.0, 41.9, 67.1, 71.5, 72.3, 100.0, 118.2, 125.5, 128.2 (2C), 128.4 (2C), 134.8, 142.8 ppm. HR-ESI-TOF-MS: *m*/*z* 439.3189 ($[MNa]^+$, calculated for $C_{27}H_{44}O_3Na$, 439.3188).

4.2.13 (*S*)-7-((4*S*,6*R*)-2,2-Dimethyl-6-(6-phenylhexyl)-1,3-dioxan-4-yl)-7-methyloct-1-en-4-yl methanesulfonate (21)

To a suspension of **20** (49.4 mg, 0.119 mmol) and $Me_3N \cdot HCl$ (1.4 mg, 15 μmol, 0.12 equiv.) in CH_2Cl_2 (120 μL) were added Et_3N (25 μL, 0.18 mmol, 1.5 equiv.) and methanesulfonyl chloride (14 μL, 0.18 mmol, 1.5 equiv.) at 0 °C. After stirring for 2 h at the same temperature, the reaction mixture was diluted with CH_2Cl_2 (2.0 mL). The resulting mixture was poured into EtOAc (10 mL) and H_2O (10 mL). After the organic layer was separated, the aqueous layer was extracted with EtOAc (10 mL × 2). The combined organic layers were washed with brine, dried over Na_2SO_4, filtered, and concentrated *in vacuo*. The residue was purified by column chromatography (silica gel, 3%→5% EtOAc/toluene) to afford **21** (51.6 mg, 0.104 mmol, 87%) as a colorless oil. $[\alpha]_D$: −24 (*c* 0.30, $CHCl_3$, 24.0 °C). ^{1}H NMR (500 MHz, 294 K, $CDCl_3$, 0.030 M): δ 0.80 (3H, s), 0.84 (3H, s), 1.26–1.51 (17H, m), 1.58–1.74 (5H, m), 2.46–2.48 (2H, m), 2.60 (2H, t, *J* = 7.7 Hz), 2.99 (3H, s), 3.46 (1H, dd, *J* = 9.7, 6.3 Hz), 3.64 (1H, m), 4.67 (1H, quintet, *J* = 6.0 Hz), 5.15–5.18 (2H, m), 5.79 (1H, ddt, *J* = 17.5, 10.3, 7.2 Hz), 7.16–7.18 (3H, m), 7.26–7.29 (2H, m) ppm. ^{13}C NMR (125 MHz, 294 K, $CDCl_3$, 0.030 M): δ 22.2, 22.4, 24.3, 24.6, 25.4, 28.6, 29.2, 29.4, 31.4, 33.5, 33.6, 35.6, 35.9, 36.0, 38.7, 39.0, 67.1, 72.2, 83.7, 100.1, 119.0, 125.5, 128.2 (2C), 128.4 (2C), 132.5, 142.8 ppm. HR-ESI-TOF-MS: *m*/*z* 517.2971 ($[MNa]^+$, calculated for $C_{28}H_{46}O_5NaS$, 517.2964).

4.2.14 (4*S*,8*S*,10*R*)-8,10-Dihydroxy-7,7-dimethyl-16-phenylhexadec-1-en-4-yl methanesulfonate (6)

To a solution of **21** (48.3 mg, 0.0976 mmol) in THF (1.0 mL) was added 10% aqueous HCl (1.0 mL), and the reaction mixture was stirred for 1.5 h at room temperature. The reaction was diluted with H_2O (10 mL) and then extracted with CH_2Cl_2 (10 mL × 3). The combined organic layers were washed with brine, dried over Na_2SO_4, filtered, and concentrated *in vacuo*. The residue was purified by column chromatography (silica gel, 40% EtOAc/hexane) to afford **6** (39.2 mg, 86.2 μmol, 88%) as a colorless oil. $[\alpha]_D$: −16 (*c* 0.29, $CHCl_3$, 24.1 °C). ^{1}H NMR (500 MHz, 295 K, $CDCl_3$, 0.012 M): δ 0.85 (3H, s), 0.88 (3H, s), 1.25–1.79 (16H, m), 1.90–1.96 (2H, m), 2.48 (2H, t, *J* = 6.3 Hz), 2.60 (2H, t, *J* = 7.7 Hz), 3.00 (3H, s), 3.67 (1H, dd, *J* = 10.5, 2.0 Hz), 3.90 (1H, m), 4.73 (1H, quintet, *J* = 6.0 Hz), 5.15–5.19 (2H, m), 5.79 (1H, ddt, *J* = 17.5, 10.3, 7.2 Hz), 7.16–7.18 (3H, m), 7.26–7.29 (2H, m) ppm. ^{13}C NMR (125 MHz, 295 K, $CDCl_3$, 0.048 M): δ 22.7, 22.9, 25.9, 28.4, 29.2, 29.4, 31.4, 33.2, 35.9, 36.7, 36.8, 37.0, 38.7, 38.7, 70.0, 74.1, 83.4, 119.0, 125.6, 128.2 (2C), 128.4 (2C), 132.5, 142.8 ppm. HR-ESI-TOF-MS: *m*/*z* 477.2654 ($[MNa]^+$, calculated for $C_{25}H_{42}O_5NaS$, 477.2651).

4.2.15 (*R*)-1-((2*S*,6*R*)-6-Allyl-3,3-dimethyltetrahydro-2*H*-pyran-2-yl)-8-phenyloctan-2-ol (4)

To a suspension of NaH (60% in oil, 17.0 mg, 0.425 mmol, 5.0 equiv., washed with hexane (0.5 mL × 3)) in THF (1.3 mL) was added a solution of **6** (38.6 mg, 0.0849 mmol) in THF (2.6 mL) at 0 °C. The mixture was allowed to warm to room temperature and stirred for 24 h. The reaction was quenched with saturated aqueous NH_4Cl (2.0 mL), and the resulting mixture was extracted with EtOAc (5 mL × 3). The combined organic layers were washed with brine, dried over Na_2SO_4, filtered, and concentrated *in vacuo*. The residue was purified by column chromatography (silica gel, 10% EtOAc/hexane) to afford **4** (22.9 mg, 63.9 μmol, 75%) as a colorless oil. $[\alpha]_D$: −38.1 (*c* 1.33, $CHCl_3$, 18.4 °C). ^{1}H NMR (500 MHz, 295 K, $CDCl_3$, 0.040 M): δ 0.86 (3H, s), 0.94 (3H, s), 1.30–1.52 (12H, m), 1.59–1.77 (4H, m), 2.19 (1H, m), 2.33 (1H, d, *J* = 5.4 Hz), 2.51 (1H, m), 2.60 (2H, t, *J* = 7.7 Hz), 3.61 (1H, dd, *J* = 11.5, 2.3 Hz), 3.74–3.82 (2H, m), 5.07 (1H, dd, *J* = 10.3, 1.0 Hz), 5.12 (1H, dd, *J* = 16.9, 0.5 Hz), 5.84 (1H, ddt, *J* = 17.2, 10.3, 6.9 Hz), 7.16–7.18 (3H, m), 7.26–7.29 (2H, m) ppm. ^{13}C NMR (125 MHz, 295 K, $CDCl_3$, 0.040 M): δ 22.3, 25.6, 25.9, 27.3, 29.3, 29.5, 31.5, 32.1, 33.3, 34.7, 35.9, 37.3 (2C), 68.3, 70.8, 74.9, 116.8, 125.5,

128.2 (2C), 128.4 (2C), 135.9, 142.9 ppm. HR-ESI-TOF-MS: *m*/*z* 381.2774 ([MNa]$^+$, calculated for $C_{24}H_{38}O_2Na$, 381.2770).

4.2.16 (*R*)-1-((2S,6R)-6-Allyl-3,3-dimethyltetrahydro-2*H*-pyran-2-yl)-8-phenyloctan-2-yl (*R*)-4-(benzyloxy)-3-((*tert*-butyldimethylsilyl)oxy)butanoate (22)

To a solution of carboxylic acid **5** (50.0 mg, 0.154 mmol, 2.4 equiv.) in toluene (0.7 mL) were added Et_3N (17.8 μL, 0.128 mmol, 2.0 equiv.) and 2,4,6-trichlorobenzoyl chloride (20.0 μL, 0.128 mmol, 2.0 equiv.). After stirring for 2 h at room temperature, a supernatant of the resulting suspension was added to a solution of **4** (22.9 mg, 0.0639 mmol) and 4-dimethylaminopyridine (15.6 mg 0.128 mmol, 2.0 equiv.) in toluene (0.7 mL) heated to 50 °C. After stirring for 1.5 h at 50 °C, the reaction was quenched with H_2O (10 mL). The mixture was cooled to room temperature and the resulting mixture was then extracted with EtOAc (20 mL × 3). The combined organic layers were washed with brine, dried over Na_2SO_4, filtered, and concentrated *in vacuo*. The residue was purified by column chromatography (silica gel, 2.5%→5% EtOAc/hexane) to afford **22** (39.9 mg, 60.0 μmol, 94%) as a colorless oil. $[\alpha]_D$: −21 (*c* 0.53, $CHCl_3$, 15.7 °C). ^{1}H NMR (500 MHz, 295 K, $CDCl_3$, 0.026 M): δ 0.06 (6H, s), 0.83 (3H, s), 0.86 (9H, s), 0.92 (3H, s), 1.27–1.42 (9H, m), 1.54–1.71 (7H, m), 2.18 (1H, m), 2.36 (1H, m), 2.46 (1H, dd, *J* = 15.7, 6.9 Hz), 2.57–2.62 (3H, m), 3.33 (1H, dd, *J* = 10.3, 2.3 Hz), 3.42 (1H, dd, *J* = 9.7, 5.4 Hz), 3.47 (1H, dd, *J* = 9.7, 5.4 Hz), 3.65–3.68 (1H, m), 4.31 (1H, quintet, *J* = 5.4 Hz), 4.53 (2H, s), 4.94 (1H, m), 5.00–5.05 (2H, m), 5.79 (1H, ddt, *J* = 17.2, 10.0, 6.9 Hz), 7.16–7.17 (3H, m), 7.25–7.35 (7H, m) ppm. ^{13}C NMR (125 MHz, 295 K, $CDCl_3$, 0.026 M): δ −4.9, −4.6, 18.1, 22.3, 25.2, 25.2, 25.8 (3C), 27.3, 29.2, 29.5, 31.5, 32.1, 32.9, 33.2, 35.0, 36.0, 37.2, 40.2, 68.4, 70.8, 72.2, 73.3, 74.0, 75.0, 116.6, 125.6, 127.5, 127.5 (2C), 128.2 (2C), 128.3 (2C), 128.4 (2C), 135.5, 138.3, 142.8, 170.9 ppm. HR-ESI-TOF-MS: *m*/*z* 687.4432 ([MNa]$^+$, calculated for $C_{41}H_{64}O_5NaSi$, 687.4421).

4.2.17 (*R*)-1-((2*S*,6*R*)-6-Allyl-3,3-dimethyltetrahydro-2H-pyran-2-yl)-8-phenyloctan-2-yl(*R*)-4-(benzyloxy)-3-hydroxybutanoate (23)

To a solution of **22** (8.1 mg, 12 μmol) in THF (1.6 mL) was added HF·pyridine (205 μL) at 0 °C. After warming to room temperature, the reaction mixture was stirred for 25 h. The reaction was quenched with saturated aqueous $NaHCO_3$ (10 mL). The resulting mixture was extracted with EtOAc (15 mL × 3). The combined organic layers were washed with brine, dried over Na_2SO_4, filtered, and concentrated *in vacuo*. The residue was purified by column chromatography (silica gel, 10%→15% EtOAc/hexane) to afford **23** (6.3 mg, 11 μmol, 94%) as a colorless oil. $[\alpha]_D$: −28.4 (*c* 0.45, $CHCl_3$, 19.7 °C). ^{1}H NMR (500 MHz, 295 K, $CDCl_3$, 0.022 M): δ 0.84 (3H, s), 0.94 (3H, s), 1.25–1.43 (9H, m), 1.51–1.73 (7H, m), 2.18 (1H, m), 2.36 (1H, m), 2.51 (1H, dd, *J* = 16.0, 8.6 Hz), 2.56 (1H, dd, *J* = 16.0, 4.3 Hz), 2.59 (2H, t, *J* = 7.4 Hz), 3.25 (1H, d, *J* = 4.3 Hz), 3.37 (1H, dd, *J* =10.9, 2.3 Hz), 3.50 (2H, d, *J* = 5.4 Hz), 3.66 (1H, m), 4.24 (1H, m), 4.56 (2H, s), 5.00–5.06 (3H, m), 5.79 (1H, ddt, *J* = 17.2, 10.0, 6.9 Hz), 7.15–7.18 (3H, m), 7.25–7.37 (7H, m) ppm. ^{13}C NMR (125 MHz, 295 K, $CDCl_3$, 0.022 M): δ 22.6, 25.2, 25.3, 27.2, 29.2, 29.4, 31.4, 32.0, 32.6, 33.0, 34.9, 35.9, 37.4, 38.9, 67.3, 70.9, 72.1, 73.2, 73.4, 75.0, 116.7, 125.6, 127.7 (2C), 127.7, 128.2 (2C), 128.4 (2C), 128.4 (2C), 135.3, 138.0, 142.8, 171.6 ppm. HR-ESI-TOF-MS: *m*/*z* 573.3566 ([MNa]$^+$, calculated for $C_{35}H_{50}O_5Na$, 573.3556).

4.2.18 2-((2*R*,6*S*)-6-((*R*)-2-(((*R*)-4-(Benzyloxy)-3-hydroxybutanoyl)oxy)-8-phenyloctyl)-5,5-dimethyltetrahydro-2*H*-pyran-2-yl)acetic acid (24)

To a suspension of $NaIO_4$ (18.3 mg, 85.6 μmol, 8.0 equiv.) in pH 7.2 phosphate buffer (0.9 mL) was added $KMnO_4$ (1.7 mg, 0.011 mmol, 1.0 equiv.) in one portion. After stirring for 15 min at room temperature, the mixture was added to a solution of alcohol **23** (5.9 mg, 11 μmol) in *t*-BuOH (0.9 mL). The reaction

mixture was stirred for 45 min at room temperature. The reaction was quenched with $Na_2S_2O_3$ (5.1 mg), and the resulting mixture was poured into EtOAc (10 mL) and H_2O (10 mL). After the organic layer was separated, the aqueous layer was extracted with EtOAc (10 mL × 3). The combined organic layers were washed with brine, dried over Na_2SO_4, filtered, and concentrated *in vacuo*. The residue was purified by column chromatography (silica gel, 40%→50% EtOAc/hexane containing 0.5% AcOH) to afford **24** (4.5 mg, 7.9 μmol, 74%) as a colorless oil. $[\alpha]_D$: −31 (*c* 0.19, $CHCl_3$, 20.7 °C). ^{1}H NMR (500 MHz, 294 K, $CDCl_3$, 0.016 M): δ 0.85 (3H, s), 0.95 (3H, s), 1.25–1.30 (6H, m), 1.39–1.65 (8H, m), 1.69–1.81 (2H, m), 2.42 (1H, dd, *J* = 14.9, 4.9 Hz), 2.50 (1H, dd, *J* = 16.0, 8.6 Hz), 2.57 (1H, dd, *J* = 16.0, 4.0 Hz), 2.58 (2H, t, *J* = 8.0 Hz), 2.68 (1H, dd, *J* = 14.9, 8.9 Hz), 3.41 (1H, dd, *J* = 11.2, 2.0 Hz), 3.50 (2H, d, *J* = 5.4 Hz), 4.15 (1H, m), 4.25 (1H, m), 4.56 (2H, s), 5.01 (1H, m), 7.15–7.18 (3H, m), 7.25–7.37 (7H, m) ppm. ^{13}C NMR (125 MHz, 294 K, $CDCl_3$, 0.016 M): δ 22.6, 25.0, 25.8, 27.1, 29.2, 29.4, 31.4, 31.9, 32.4, 32.8, 34.8, 35.9, 38.1, 38.8, 67.3, 67.9, 71.8, 73.2, 73.4, 75.1, 125.6, 127.8 (3C), 128.2 (2C), 128.4 (4C), 137.8, 142.8, 172.0, 173.4 ppm. HR-ESI-TOF-MS: *m*/*z* 591.3298 ($[MNa]^+$, calculated for $C_{34}H_{48}O_7Na$, 591.3298).

4.2.19 (1*R*,5*R*,9*R*,11*S*)-5-((Benzyloxy)methyl)-12,12-dimethyl-9-(6-phenylhexyl)-4,8,15-trioxabicyclo[9.3.1]pentadecane-3,7-dione (25)

To a solution of **24** (15.8 mg, 27.8 μmol) in toluene (3.0 mL) were added Et_3N (116 μL, 0.833 mmol, 30 equiv.) and 2,4,6-trichlorobenzoyl chloride (87 μL, 0.56 mmol, 20 equiv.). After stirring for 1.5 h at room temperature, the mixture was diluted with toluene (16 mL). The supernatant of the mixture was added dropwise over 3 h to a solution of 4-dimethylaminopyridine (170 mg, 1.39 mmol, 50 equiv.) in toluene (30 mL). After stirring for 20 h at room temperature, the reaction was quenched with saturated aqueous $NaHCO_3$ (50 mL). The resulting mixture was extracted with EtOAc (50 mL × 3). The combined organic layers were washed with brine, dried over Na_2SO_4, filtered, and concentrated *in vacuo*. The residue was purified by column chromatography (silica gel, 10%→15% EtOAc/hexane) to afford **25** (10.5 mg, 19.1 μmol, 69%) as a colorless oil. $[\alpha]_D$: +2.6 (*c* 0.53, $CHCl_3$, 28.8 °C). ^{1}H NMR (500 MHz, 294 K, $CDCl_3$, 0.038 M): δ 0.79 (3H, s), 1.03 (3H, s), 1.19–1.51 (12H, m), 1.58–1.61 (2H, m), 1.76 (1H, m), 2.29 (1H, ddd, *J* = 14.9, 12.3, 2.6 Hz), 2.42 (1H, dd, *J* = 13.5, 3.2 Hz), 2.50 (1H, m), 2.59 (2H, t, *J* = 7.7 Hz), 2.71 (1H, dd, *J* = 17.5, 2.9 Hz), 2.84 (1H, dd, *J* = 17.5, 10.6 Hz), 3.53 (1H, dd, *J* = 10.3, 5.2 Hz), 3.59 (1H, dd, *J* = 10.3, 4.6 Hz), 3.63 (1H, m), 4.01 (1H, m), 4.50 and 4.57 (2H, ABq, *J* = 12.0 Hz), 4.97 (1H, m), 5.38 (1H, m), 7.15–7.18 (3H, m), 7.25–7.36 (7H, m) ppm. ^{13}C NMR (125 MHz, 294 K, $CDCl_3$, 0.038 M): δ 25.0, 26.1, 26.7, 27.1, 28.4, 29.1, 29.2, 31.2, 31.4, 32.0, 32.4, 35.9, 37.0, 41.0, 67.3, 68.2, 70.5, 73.3, 73.8, 75.9, 125.5, 127.7 (2C), 127.8, 128.1 (2C), 128.4 (2C), 128.4 (2C), 137.7, 142.8, 170.1, 170.4 ppm. HR-ESI-TOF-MS: *m*/*z* 573.3198 ($[MNa]^+$, calculated for $C_{34}H_{46}O_6Na$, 573.3192).

4.2.20 (1*R*,5*R*,9*R*,11*S*)-5-(Hydroxymethyl)-12,12-dimethyl-9-(6-phenylhexyl)-4,8,15-trioxabicyclo[9.3.1]pentadecane-3,7-dione (3)

To a solution of **25** (9.2 mg, 17 μmol) in EtOH (2.0 mL) was added 10% Pd/C (4.6 mg). The reaction mixture was stirred for 20 h at room temperature under H_2 atmosphere. The reaction mixture was then filtered, and the filtrate was concentrated *in vacuo*. The residue was purified by HPLC (column, YMC-pack ODS-AM AM12S05-1520WT; solvent, 87.5% MeOH/H_2O; flow rate, 8.0 mL/min; UV detector, 254 nm; retention time, 12.4 min) to afford **3** (5.3 mg, 12 μmol, 69%) as a white crystal. $[\alpha]_D$: +3.9 (*c* 0.60, $CHCl_3$, 27.3 °C). ^{1}H NMR (500 MHz, 294 K, $CDCl_3$, 0.023 M): δ 0.79 (3H, s, H-23), 1.04 (3H, s, H-22), 1.20–1.60 (14H, m, H-4, H-5, H-8β, H-10a, H-11, H-12, H-13, H-14), 1.74–1.81 (1H, m, H-10b), 2.07 (1H, br s, 27-OH), 2.33 (1H, ddd, *J* = 15.2, 11.5, 2.9 Hz, H-8α), 2.45 (1H, dd, *J* = 13.7, 3.4 Hz, H-2β), 2.52 (1H, m, H-2α), 2.60 (2H, t, *J* = 7.7 Hz, H-15), 2.70 (1H, dd, *J* = 17.2, 3.4 Hz, H-25β), 2.78 (1H, dd, *J* = 17.2, 10.0 Hz, H-25α), 3.64 (1H, m, H-7), 3.69–3.77 (2H, m, H-27), 4.02 (1H, m, H-3), 4.98 (1H, m, H-9), 5.29 (1H, m, H-26), 7.16–7.19 (3H, m, H-17, H-19, H-21), 7.26–7.29 (2H, m, H-18, H-20) ppm.

^{13}C NMR (125 MHz, 294 K, $CDCl_3$, 0.023 M): δ 25.5 (C-23), 26.1 (C-12), 26.8 (C-4), 27.1 (C-22), 28.3 (C-8), 29.1 (C-13), 29.2 (C-11), 31.3 (C-10), 31.4 (C-14), 32.1 (C-6), 32.3 (C-5), 35.9 (C-15), 36.5 (C-25), 41.2 (C-2), 64.3 (C-27), 67.1 (C-3), 70.6 (C-26), 74.0 (C-9), 76.0 (C-7), 125.6 (C-19), 128.2 (2C, C-18, C-20), 128.4 (2C, C-17, C-21), 142.8 (C-16), 169.9 (C-24), 171.2 (C-1) ppm. HR-ESI-TOF-MS: m/z 483.2720 ($[MNa]^+$, calculated for $C_{27}H_{40}O_6Na$, 483.2723).

4.3 Molecular modeling

4.3.1 Conformational search of 3

The three-dimensional structure of **3** was built using Avogadro (version 1.2.0).[60] Simulated annealing was carried out using the GROMACS program (version 2021.3)[57] with a general AMBER force field 2 (GAFF2) in the AmberTools21 package.[61] An aromatic side chain at C9 was replaced with a ethyl group to simplify calculation. All bonds were constrained using the LINCS algorithm. The time step was set to 1 fs. The annealing temperature was initially set to 1,500 K and the temperature was kept constant for 2 ps. The temperature was linearly dropped to 100 K over 1 ps and then to 0 K over 1 ps, and kept at the same temperature for 1 ps. This 5-ps cycle was repeated 1,000 times to give conformer library. Two possible conformers A and B were selected and optimized at the M06-2X/aug-cc-pVTZ level of theory with polarizable continuum model using the integral equation formalism (IEFPCM) solvent model with chloroform solvent using the Gaussian16 program.[62]

4.3.2 MD simulation

MD simulation and MM/PBSA calculation were performed as described previously.[30] All MD simulation were performed using the GROMACS program (version 2021.3). MM/PBSA calculation and energy decomposition per residue were performed by the MMPBSA.py.MPI[63] module in AmberTools21. The final coordinate of the protein/ligand complex in each replica was analyzed by the PPM server[56] to estimate $\Delta G^{\circ}_{transfer}$.

4.4 Inhibition of specific binding of [^{3}H]PDBu to the PKC C1 peptides

The binding of [^{3}H]PDBu to the PKCα-C1A and δ-C1B peptides was evaluated by the procedure of Sharkey and Blumberg[52] with modification as reported previously[48] using 50 mM Tris-maleate buffer (pH 7.4 at 4 °C), 40 nM α-C1A peptide or 13.8 nM δ-C1B peptide, 20 nM [^{3}H]PDBu (13.92 Ci/mmol accounting for radioactive decay), 50 μg/mL 1,2-dioleoyl-*sn*-glycero-3-phospho-L-serine (Funakoshi), 3 mg/mL bovine γ-globulin (Sigma), and various concentrations of **3**. Binding affinity was evaluated on the basis of the concentration required to cause 50% inhibition of the specific binding of [^{3}H]PDBu, IC_{50}, which was calculated by logit analysis using Microsoft Excel (Microsoft, USA). The binding inhibition constant, K_i, was calculated by the equation of Goldstein and Barrett,[53] $K_i = IC_{50}/(2[L_{50}]/[L_0] - 1 + [L_{50}]/K_d)$, where $[L_{50}]$ and $[L_0]$ are the free concentration of [^{3}H]PDBu at 50% and 0% inhibition, respectively. The mean K_i values and the 95% confidence intervals (based on t-distribution) were calculated on the logarithm scale and converted to the nanomolar unit.

4.5 Measurements of cell growth inhibition

Cell growth inhibitory activity was evaluated toward a panel of 39 human cancer cell lines established by Yamori and colleagues.[59] In brief, the cells were plated in 96-well plates in RPMI 1640 medium supplemented with 5% fetal bovine serum and allowed to attach overnight. The cells were incubated with the test compound for 48 h. Cell growth was estimated by the sulforhodamine B assay. Absorbance for the control well (C) and test well (T) was measured at 525 nm along with that for the test well at time 0 (T_0).

Cell growth inhibition (% growth) by each concentration of drug (10^{-8}, 10^{-7}, 10^{-6}, 10^{-5}, and 10^{-4} M) was calculated as $100[(T - T_0)/(C - T_0)]$ (if $T > T_0$) or $100[(T\text{-}T_0)/(T_0)]$ (if $T < T_0$) using the mean of duplicate points.

Declaration of conflict of interest

The authors have no conflicts of interest to declare.

Acknowledgements

This work was supported by JSPS KAKENHI Grant No.17H06405 (to K.I. and R.C.Y.) and the Molecular Profiling Committee, Grant-in-Aid for Scientific Research on Innovative Areas "Advanced Animal Model Support (AdAMS)" from the Ministry of Education, Culture, Sports, Science and Technology, Japan (JSPS KAKENHI Grant No. JP 16H06276). The DFT calculation was performed using Research Center for Computational Science, Okazaki, Japan (Project: 21-IMS-C185).

Supplementary material

^{1}H, ^{13}C, and 2-D NMR spectra, growth inhibitory assay data for human cancer cell lines, Cartesian coordinates for the calculated conformers and the docked complexes, and the output of the DFT calculations associated with this article are available online at URL: `https://doi.org/10.1016/j.bmc.2022.116988`.

References

[1] Helen J. Mackay and Christopher J. Twelves. Targeting the protein kinase C family: are we there yet? *Nature reviews. Cancer*, 7(7):554–562, 2007.

[2] Michael Fahrmann. Targeting protein kinase C (PKC) inphysiology and cancer of the gastric cell system. *Current Medicinal Chemistry*, 15(12):1175–1191, 2008.

[3] Alessia Pascale, Marialaura Amadio, Stefano Govoni, and Fiorenzo Battaini. The aging brain, a key target for the future: The protein kinase C involvement. *Pharmacological Research*, 55(6):560–569, 2007.

[4] Kenneth A. Roebuck, De Sheng Gu, and Martin F. Kagnoff. Activating protein-1 cooperates with phorbol ester activation signals to increase HIV-1 expression. *AIDS*, 10(8):819–26, 1996.

[5] Alexandra C. Newton. Protein kinase C: Structure, function, and regulation. *Journal of Biological Chemistry*, 270(48):28495–28498, 1995.

[6] Yasutomi Nishizuka. Protein kinase C and lipid signaling for sustained cellular responses. *The FASEB Journal*, 9(7):484–496, 1995.

[7] Susan Young, Peter J. Parker, Axel Ullrich, and Silvia Stabel. Down-regulation of protein kinase C is due to an increased rate of degradation. *Biochemical Journal*, 244(3):775–779, jun 1987.

[8] Gurdip Hansra, Frederic Bornancin, Richard Whelan, Brian A. Hemmings, and Peter J. Parker. 12-*O*-Tetradecanoylphorbol-13-acetate-induced dephosphorylation of protein kinase Cα correlates with the presence of a membraneassociated protein phosphatase 2A heterotrimer. *Journal of Biological Chemistry*, 271(51):32785–32788, 1996.

[9] Peter M. Blumberg. In vitro studies on the mode of action of the phorbol esters, potent tumor promoters: Part 1. *Critical Reviews in Toxicology*, 8(2):153–197, 1980.

[10] T. J. Nelson and D. L. Alkon. Neuroprotective versus tumorigenic protein kinase C activators. *Trends in Biochemical Sciences*, 34(3):136–145, 2009.

[11] Paul M. Choi, Kam-Meng Tchou-Wong, and I. Bernard Weinstein. Overexpression of protein kinase C in HT29 colon cancer cells causes growth inhibition and tumor suppression. *Molecular and Cellular Biology*, 10(9):4650–4657, 1990.

[12] Henrik Oster and Michael Leitges. Protein kinase C α but not PKCζ suppresses intestinal tumor formation in $Apc^{Min/+}$ mice. *Cancer Research*, 66(14):6955–6963, 2006.

[13] A. M. D'Costa, J. K. Robinson, T. Maududi, V. Chaturvedi, B. J. Nickoloff, and M. F. Denning. The proapoptotic tumor suppressor protein kinase C-δ is lost in human squamous cell carcinomas. *Oncogene*, 25(3):378–386, jan 2006.

[14] Peter J. Reddig, Nancy E. Dreckschimdt, Helga Ahrens, Robita Simsiman, Ching Ping Tseng, Jun Zou, Terry D. Oberley, and Ajit K. Verma. Transgenic mice overexpressing protein kinase Cδ in the epidermis are resistant to skin tumor promotion by 12-*O*-tetradecanoylphorbol-13-acetate. *Cancer Research*, 59(22):5710–5718, 1999.

[15] José G. Hernández-Maqueda, Luis Bernardo Luna-Ulloa, Paula Santoyo-Ramos, M. Cristina Castañeda-Patlán, and Martha Robles-Flores. Protein kinase C delta negatively modulates canonical Wnt pathway and cell proliferation in colon tumor cell lines. *PLoS ONE*, 8(3):e58540, 2013.

[16] Corina E. Antal, Andrew M. Hudson, Emily Kang, Ciro Zanca, Christopher Wirth, Natalie L. Stephenson, Eleanor W. Trotter, Lisa L. Gallegos, Crispin J. Miller, Frank B. Furnari, Tony Hunter, John Brognard, and Alexandra C. Newton. Cancer-associated protein kinase C mutations reveal kinase's role as tumor suppressor. *Cell*, 160(3):489–502, 2015.

[17] M. G. Kazanietz, L. B. Areces, A. Bahador, H. Mischak, J. Goodnight, J. F. Mushinski, and P. M. Blumberg. Characterization of ligand and substrate specificity for the calcium-dependent and calcium-independent protein kinase C isozymes. *Molecular pharmacology*, 44(2):298–307, aug 1993.

[18] Joydip Das and Ghazi M. Rahman. C1 domains: Structure and ligand-binding properties. *Chemical Reviews*, 114(24):12108–12131, 2014.

[19] Mariana Cooke, Xiaoling Zhou, Victoria Casado-Medrano, Cynthia Lopez-Haber, Martin J. Baker, Rachana Garg, Jihyae Ann, Jeewoo Lee, Peter M. Blumberg, and Marcelo G. Kazanietz. Characterization of AJH-836, a diacylglycerol-lactone with selectivity for novel PKC isozymes. *Journal of Biological Chemistry*, 293(22):8330–8834, 2018.

[20] Ryo C. Yanagita, Yu Nakagawa, Nobuhiro Yamanaka, Kaori Kashiwagi, Naoaki Saito, and Kazuhiro Irie. Synthesis, conformational analysis, and biological evaluation of 1-hexylindolactam-V10 as a selective activator for novel protein kinase C isozymes. *Journal of Medicinal Chemistry*, 51(1):46–56, 2008.

[21] Yu Nakagawa, Ryo C. Yanagita, Naoko Hamada, Akira Murakami, Hideyuki Takahashi, Naoaki Saito, Hiroshi Nagai, and Kazuhiro Irie. A simple analogue of tumor-promoting aplysiatoxin is an antineoplastic agent rather than a tumor promoter: Development of a synthetically accessible protein kinase C activator with bryostatin-like activity. *Journal of the American Chemical Society*, 131(22):7573–7579, 2009.

[22] Ryo C. Yanagita, Hiroaki Kamachi, Keisuke Tanaka, Akira Murakami, Yu Nakagawa, Harukuni Tokuda, Hiroshi Nagai, and Kazuhiro Irie. Role of the phenolic hydroxyl group in the biological activities of simplified analogue of aplysiatoxin with antiproliferative activity. *Bioorganic and Medicinal Chemistry Letters*, 20(20):6064–6066, 2010.

[23] Masayuki Kikumori, Ryo C. Yanagita, Harukuni Tokuda, Nobutaka Suzuki, Hiroshi Nagai, Kiyotake Suenaga, and Kazuhiro Irie. Structure-activity studies on the spiroketal moiety of a simplified analogue of debromoaplysiatoxin with antiproliferative activity. *Journal of Medicinal Chemistry*, 55(11):5614–5626, 2012.

[24] Masayuki Kikumori, Ryo C. Yanagita, Harukuni Tokuda, Kiyotake Suenaga, Hiroshi Nagai, and Kazuhiro Irie. Structural optimization of 10-methyl-aplog-1, a simplified analog of debromoaplysiatoxin, as an anticancer lead. *Bioscience, Biotechnology, and Biochemistry*, 80(2):221–231, 2016.

[25] Yoshiki Ashida, Ryo C. Yanagita, Yasuhiro Kawanami, Mutsumi Okamura, Shingo Dan, and Kazuhiro Irie. Synthesis, conformation, and biological activities of a des-A-ring analog of 18-deoxy-aplog-1, a simplified analog of debromoaplysiatoxin. *Heterocycles*, 99(2):942–957, 2019.

[26] Yoshinori Kato and Paul J. Scheuer. Aplysiatoxin and debromoaplysiatoxin, constituents of the marine mollusk *Stylocheilus longicauda*. *Journal of the American Chemical Society*, 96(7):2245–2246, apr 1974.

[27] Henner Knust and Reinhard W. Hoffmann. A case study in conformation design: Learning by doing. *Chemical Record*, 2(6):405–418, 2002.

[28] Henner Knust and Reinhard W. Hoffmann. Synthesis and conformational analysis of macrocyclic dilactones mimicking the pharmacophore of aplysiatoxin. *Helvetica Chimica Acta*, 86(6):1871–1893, 2003.

[29] Takumi Kobayashi, Ryo C. Yanagita, and Kazuhiro Irie. Synthesis and biological activities of simplified aplysiatoxin analogs focused on the CH/π interaction. *Bioorganic and Medicinal Chemistry Letters*, 30(24):127657, 2020.

[30] Atsuko Gonda, Koji Takada, Ryo C. Yanagita, Shingo Dan, and Kazuhiro Irie. Effects of side chain length of 10-methyl-aplog-1, a simplified analog of debromoaplysiatoxin, on PKC binding, anti-proliferative, and pro-inflammatory activities. *Bioscience, Biotechnology, and Biochemistry*, 85(1):168–180, 2021.

[31] Koutaro Hayakawa, Yusuke Hanaki, Harukuni Tokuda, Ryo C. Yanagita, Yu Nakagawa, Mutsumi Okamura, Shingo Dan, and Kazuhiro Irie. Synthesis and Biological Activities of Acetal Analogs at Position 3 of 10-Methyl-Aplog-1, a Potential Anti-Cancer Lead Derived from Debromoaplysiatoxin. *Heterocycles*, 97(1):478–492, 2018.

[32] Robert D. Walkup and Raymond T. Cunningham. Studies on the syntheses of the aplysiatoxins: Synthesis of a selectively-protected form of the C_{27}–C_{30} (dihydroxybutanoate) moiety of oscillatoxin A. *Tetrahedron Letters*, 28(35):4019–4022, jan 1987.

[33] Naoya Ichimaru, Masatoshi Murai, Nobuyuki Kakutani, Junko Kako, Atsushi Ishihara, Yoshiaki Nakagawa, Takaaki Nishioka, Takao Yagi, and Hideto Miyoshi. Synthesis and characterization of new piperazine-type inhibitors for mitochondrial NADH-ubiquinone oxidoreductase (complex I). *Biochemistry*, 47(40):10816–10826, 2008.

[34] Junji Inanaga, Kuniko Hirata, Hiroko Saeki, Tsutomu Katsuki, and Masaru Yamaguchi. A rapid esterification by means of mixed anhydride and its application to large-ring lactonization. *Bulletin of the Chemical Society of Japan*, 52(7):1989–1993, 1979.

[35] Nadiah Mad Nasir, Kristaps Ermanis, and Paul A. Clarke. Strategies for the construction of tetrahydropyran rings in the synthesis of natural products. *Organic and Biomolecular Chemistry*, 12(21):3323–3335, 2014.

[36] Kristaps Ermanis, Yin Ting Hsiao, Uğur Kaya, Alan Jeuken, and Paul A. Clarke. The stereodivergent formation of 2,6-*cis* and 2,6-*trans*-tetrahydropyrans: experimental and computational investigation of the mechanism of a thioester oxy-Michael cyclization. *Chemical Science*, 8(1):482–490, 2017.

[37] Carlo Bonini, Lucia Chiummiento, Maddalena Pullez, Guy Solladié, and Françoise Colobert. Convergent highly stereoselective preparation of the C12–C24 fragment of macrolactin A. *Journal of Organic Chemistry*, 69(15):5015–5022, 2004.

[38] Fatih M. Uckun, Chen Mao, Alexei O. Vassilev, He Huang, and Shyi Tai Jan. Structure-based design of a novel synthetic spiroketal pyran as a pharmacophore for the marine natural product Spongistatin 1. *Bioorganic and Medicinal Chemistry Letters*, 10(6):541–545, 2000.

[39] D. A. Evans, K. T. Chapman, and E. M. Carreira. Directed reduction of β-hydroxy ketones employing tetramethylammonium triacetoxyborohydride. *Journal of the American Chemical Society*, 110(11):3560–3578, may 1988.

[40] Anthony J. Mancuso, Shui Lung Huang, and Daniel Swern. Oxidation of long-chain and related alcohols to carbonyls by dimethyl sulfoxide "activated" by oxalyl chloride. *Journal of Organic Chemistry*, 43(12):2480–2482, 1978.

[41] Gary E. Keck and Dhileepkumar Krishnamurthy. Catalytic Asymmetric Allylation Reactions:(*S*)-1-(Phenylmethoxy)-4-Penten-2-ol. *Organic Syntheses*, 75:12, 1998.

[42] Richard E. Moore, Adrian J. Blackman, Chad E. Cheuk, Jon S. Mynderse, Gayle K. Matsumoto, Jon Clardy, Ronald W. Woodard, and J. Cymerman Craig. Absolute stereochemistries of the aplysiatoxins and oscillatoxin A. *The Journal of Organic Chemistry*, 49(13):2484–2489, 1984.

[43] Hideshi Nakamura, Yoshito Kishi, Maria A. Pajares, and Robert R. Rando. Structural basis of protein kinase C activation by tumor promoters. *Proceedings of the National Academy of Sciences of the United States of America*, 86(24):9672–9676, 1989.

[44] Yan Zhao and Donald G. Truhlar. The M06 suite of density functionals for main group thermochemistry, thermochemical kinetics, noncovalent interactions, excited states, and transition elements: Two new functionals and systematic testing of four M06-class functionals and 12 other function. *Theoretical Chemistry Accounts*, 120(1-3):215–241, 2008.

[45] Thom H. Dunning, Jr. Gaussian basis sets for use in correlated molecular calculations. I. The atoms boron through neon and hydrogen. *The Journal of Chemical Physics*, 90(2):1007–1023, jan 1989.

[46] Yusuke Hanaki, Yuki Shikata, Masayuki Kikumori, Natsuki Hotta, Masaya Imoto, and Kazuhiro Irie. Identification of protein kinase C isozymes involved in the anti-proliferative and pro-apoptotic activities of 10-Methyl-aplog-1, a simplified analog of debromoaplysiatoxin, in several cancer cell lines. *Biochemical and Biophysical Research Communications*, 495(1):438–445, 2018.

[47] Kazuhiro Irie, Kentaro Oie, Akifumi Nakahara, Yoshiaki Yanai, Hajime Ohigashi, Paul A. Wender, Hiroyuki Fukuda, Hiroaki Konishi, and Ushio Kikkawa. Molecular basis for protein kinase C isozyme-selective binding: The synthesis, folding, and phorbol ester binding of the cysteine-rich domains of all protein kinase C isozymes. *Journal of the American Chemical Society*, 120(36):9159–9167, 1998.

[48] Mayumi Shindo, Kazuhiro Irie, Akifumi Nakahara, Hajime Ohigashi, Hiroaki Konishi, Ushio Kikkawa, Hiroyuki Fukuda, and Paul A. Wender. Toward the identification of selective modulators of protein kinase C (PKC) isozymes: Establishment of a binding assay for PKC isozymes using synthetic C1 peptide receptors and identification of the critical residues involved in the phorbol ester binding. *Bioorganic and Medicinal Chemistry*, 9(8):2073–2081, 2001.

[49] A.F. Quest and R.M. Bell. The regulatory region of protein kinase Cγ. Studies of phorbol ester binding to individual and combined functional segments expressed as glutathione *S*-transferase fusion proteins indicate a complex mechanism of regulation by phospholipids, phorbol . *Journal of Biological Chemistry*, 269(31):20000–20012, aug 1994.

[50] Arathi Raghunath, Mia Ling, and Christer Larsson. The catalytic domain limits the translocation of protein kinase Cα in response to increases in Ca^{2+} and diacylglycerol. *Biochemical Journal*, 370(3):901–912, mar 2003.

[51] Zoltan Szallasi, Krisztina Bogi, Shiva Gohari, Tamas Biro, Peter Acs, and Peter M. Blumberg. Non-equivalent roles for the first and second zinc fingers of protein kinase Cδ. Effect of their mutation on phorbol ester-induced translocation in NIH 3T3 cells. *The Journal of Biological Chemistry*, 271(31):18299–18301, 1996.

[52] Nancy A. Sharkey and Peter M. Blumberg. Highly lipophilic phorbol esters as inhibitors of specific [^{3}H]phorbol 12,13-dibutyrate binding. *Cancer Research*, 45:19–24, 1985.

[53] A. Goldstein and Ronald W. Barrett. Ligand dissociation constants from competition binding assays: errors associated with ligand depletion. *Molecular Pharmacology*, 31(6):603–609, 1987.

[54] Garrett M. Morris, Ruth Huey, William Lindstrom, Michel F. Sanner, Richard K. Belew, David S. Goodsell, and Arthur J. Olson. AutoDock4 and AutoDockTools4: Automated Docking with Selective Receptor Flexibility. *Journal of Computational Chemistry*, 30(16):2785–2791, 2009.

[55] Jumin Lee, Xi Cheng, Jason M. Swails, Min Sun Yeom, Peter K. Eastman, Justin A. Lemkul, Shuai Wei, Joshua Buckner, Jong Cheol Jeong, Yifei Qi, Sunhwan Jo, Vijay S. Pande, David A. Case, Charles L. Brooks, Alexander D. MacKerell, Jeffery B. Klauda, and Wonpil Im. CHARMM-GUI Input Generator for NAMD, GROMACS, AMBER, OpenMM, and CHARMM/OpenMM Simulations using the CHARMM36 Additive Force Field. *Journal of Chemical Theory and Computation*, 12(1):405–413, 2016.

[56] Mikhail A. Lomize, Irina D. Pogozheva, Hyeon Joo, Henry I. Mosberg, and Andrei L. Lomize. OPM database and PPM web server: Resources for positioning of proteins in membranes. *Nucleic Acids Research*, 40(D1):D370–D376, 2012.

[57] Mark James Abraham, Teemu Murtola, Roland Schulz, Szilárd Páll, Jeremy C. Smith, Berk Hess, and Erik Lindah. Gromacs: High performance molecular simulations through multi-level parallelism from laptops to supercomputers. *SoftwareX*, 1-2:19–25, 2015.

[58] Andrei L. Lomize, Irina D. Pogozheva, Mikhail A. Lomize, and Henry I. Mosberg. The role of hydrophobic interactions in positioning of peripheral proteins in membranes. *BMC Structural Biology*, 7:1–30, 2007.

[59] Takao Yamori, Akio Matsunaga, Shigeo Sato, Kanami Yamazaki, Akiko Komi, Kazuhiro Ishizu, Izumi Mita, Hajime Edatsugi, Yasuhiro Matsuba, Kimiko Takezawa, Osamu Nakanishi, Hiroshi Kohno, Yuki Nakajima, Hironori Komatsu, Toshio Andoh, and Takashi Tsuruo. Potent antitumor activity of MS-247, a novel DNA minor groove binder, evaluated by an *in vitro* and *in vivo* human cancer cell line panel. *Cancer Research*, 59(16):4042–4049, 1999.

[60] Marcus D. Hanwell, Donald E. Curtis, David C. Lonie, Tim Vandermeersch, Eva Zurek, and Geoffrey R. Hutchison. Avogadro: an advanced semantic chemical editor, visualization, and analysis platform. *Journal of Cheminformatics*, 4:17, 2012.

[61] D. A. Case, H. M. Aktulga, K. Belfon, I. Y. Ben-Shalom, S. R. Brozell, D. S. Cerutti, T. E. Cheatham, III, G. A. Cisneros, V. W. D. Cruzeiro, T. A. Darden, R. E. Duke, G. Giambasu, M. K. Gilson, H. Gohlke, A. W. Goetz, R. Harris, S. Izadi, S. A. Izmailov, K. Kasavajhala, M. C. Kaymark, E. King, A. Kovalenko, T. Kurtzman, T. S. Lee, S. LeGrand, P. Li, C. Lin, J. Liu, T. Luchko, R. Luo, M. Machado, V. Man, M. Manathunga, K. M. Merz, Y. Miao, O. Mikhailovskii, G. Monard, H. Nguyen, K. A. O'Hearn, A. Onufriev, F. Pan, S. Pantano, R. Qi, A. Rahnamoun, D. R. Roe, A. Roitberg, C. Sagui, S. Schott-Verdugo, J. Shen, C. Simmerling, N. R. Skrynnikov, J. Smith, J. Swails, R. C. Walker, J. Wang, H. Wei, R. M. Wolf, X. Wu, Y. Xue, D. M. York, S. Zhao, and P. A. Kollman. *AMBER 2021*. University of California, San Francisco, 2021.

[62] M. J. Frisch, G. W. Trucks, H. B. Schlegel, G. E. Scuseria, M. A. Robb, J. R. Cheeseman, G. Scalmani, V. Barone, G. A. Petersson, H. Nakatsuji, X. Li, M. Caricato, A. V. Marenich, J. Bloino, B. G. Janesko, R. Gomperts, B. Mennucci, H. P. Hratchian, J. V. Ortiz, A. F. Izmaylov, J. L. Sonnenberg, D. Williams-Young, F. Ding, F. Lipparini, F. Egidi, J. Goings, B. Peng, A. Petrone, T. Henderson, D. Ranasinghe, V. G. Zakrzewski, J. Gao, N. Rega, G. Zheng, W. Liang, M. Hada, M. Ehara, K. Toyota, R. Fukuda, J. Hasegawa, M. Ishida, T. Nakajima, Y. Honda, O. Kitao, H. Nakai, T. Vreven, K. Throssell, J. A. Montgomery, Jr., J. E. Peralta, F. Ogliaro, M. J. Bearpark, J. J. Heyd, E. N. Brothers, K. N. Kudin, V. N. Staroverov, T. A. Keith, R. Kobayashi, J. Normand, K. Raghavachari, A. P. Rendell, J. C. Burant, S. S. Iyengar, J. Tomasi, M. Cossi, J. M. Millam, M. Klene, C. Adamo, R. Cammi, J. W. Ochterski, R. L. Martin, K. Morokuma, O. Farkas, J. B. Foresman, and D. J. Fox. *Gaussian 16 (Revision C.01)*. Gaussian, Inc., Wallingford CT, 2019.

[63] Bill R. Miller, III, T. Dwight McGee, Jr., Jason M. Swails, Nadine Homeyer, Holger Gohlke, and Adrian E. Roitberg. MMPBSA.py: an efficient program for end-state free energy calculations. *Journal of Chemical Theory and Computation*, 8:3314–3321, 2012.